Analysis of Temperature extremes in Canadian Cities using CMIP6 Data

A Thesis Submitted to the
College of Graduate and Postdoctoral Studies
In Partial Fulfillment of the Requirements
For the Degree of Master of science (M.Sc.)
In the Department of Civil, Geological and Environmental Engineering
University of Saskatchewan
Saskatoon

by

ROHAN KUMAR GADDAM

PERMISSION TO USE

In presenting this thesis/dissertation in partial fulfillment of the requirements for a Postgraduate degree from the University of Saskatchewan, I agree that the Libraries of this University may make it freely available for inspection. I further agree that permission for copying of this thesis/dissertation in any manner, in whole or in part, for scholarly purposes may be granted by the professor or professors who supervised my thesis/dissertation work or, in their absence, by the Head of the Department or the Dean of the College in which my thesis work was done. It is understood that any copying or publication or use of this thesis/dissertation or parts thereof for financial gain shall not be allowed without my written permission. It is also understood that due recognition shall be given to me and to the University of Saskatchewan in any scholarly use which may be made of any material in my thesis/dissertation.

DISCLAIMER

Reference in this thesis/dissertation to any specific commercial products, process, or service by trade name, trademark, manufacturer, or otherwise, does not constitute or imply its endorsement, recommendation, or favoring by the University of Saskatchewan. The views and opinions of the author expressed herein do not state or reflect those of the University of Saskatchewan and shall not be used for advertising or product endorsement purposes.

Requests for permission to copy or to make other uses of materials in this thesis/dissertation in whole or part should be addressed to:

Head of the Department of Civil, Geological and Environmental Engineering 3B48 Engineering Building,

57 Campus Drive

University of Saskatchewan Saskatoon, Saskatchewan S7N 5A9

Canada OR

Dean

College of Graduate and Postdoctoral Studies University of Saskatchewan

116 Thorvaldson Building, 110 Science Place Saskatoon, Saskatchewan S7N 5C9
Canada

ABSTRACT

An ever-growing Canadian urban population could be severely impacted by increase in temperature. Canada's mean temperature is projected to increase by 6-8°C towards the end of the 21st century. The consequence of rising temperatures is an increased likelihood of extreme temperature events like heatwaves and wildfires. The thesis aims to assess changes in extreme temperature in large Canadian urban areas. The research will help in developing mitigation measures like urban planning, which help cope with changing temperature extremes. Predicting urban temperature change will require rigorous assessment of climate models, to account for the uncertainty in projecting temperature in large urban agglomerates. CMIP6 ensemble of models, provide an opportunity for assessment of urban-based projections. The models however, would need to be of fine resolution to fully capture its variability since urban temperature is heavily influenced by local urban features that contribute to Urban heat island (UHI). Historical maximum and minimum temperature trends are analyzed for eighteen urban areas in the Canada with population greater than 250,000 and use twelve CMIP6 models of fine resolution (<1°), and four tier-one emission scenarios to assess maximum, minimum, and mean temperature trends in future. An efficient observation dataset, Serially based station data (SCDNA), was used as a reference observation dataset and a novel bias-correction technique, the Semi-Parametric Quantile Mapping method (SPQM), was used to bias-correct future temperature data. Extreme temperature events were analyzed with the help of eight selected indices of the Expert Team on Climate Change Detection and Indices (ETCCDI), across all the emission scenarios for all the cities in the study. The indices were computed for the entire future time-period (2021-2100) and for three time-slices, T1 (2021-2050), T2 (2040-2070) and T3 (2070-2100) to assess temporal variability. The magnitude, frequency, and duration of the occurrence of extreme events can be analyzed effectively using the ETCCDI indices, classified as absolute, threshold, and duration Indices and percentile indices.

The historical temperature trends in Canadian cities were found to be related with urban features like elevation and population-growth but not strongly linked with urban area. Other features of UHI were deemed essential to understand the transitioning of historical and future temperature trends in Canada. Four emission scenarios predict increasing mean temperatures in all Canadian cities, except for the optimistic emission scenario (SSP1-2.6), which shows a marginal decreasing

trend in the last quarter of the 21st century. Uneven changes are noted in all the projected indices, for example, in the annual maxima of daily maximum temperature (TXx), i.e., an increase of 0.5 °C and 0.6 °C per decade over the T1 and T2 respectively, and 0.99°C for T3 for the SSP5-8.5. Results show faster rates of warming across Canadian cities especially for the higher emission scenarios (SSP3-7.0 and SSP5-8.5).

Spatial trends of extreme temperature indices corelate with temperature trends in individual climate zones in Canada, and the cities associated with a zone, expectedly experience similar trends. Cities in the Prairies and the Great Lakes zones, experience the highest increasing trends over the absolute and threshold indices in the higher emission scenarios, whereas the cities in the Canadian coasts experience higher increasing trends in the percentile indices. Lower emission scenarios also point towards increasing spatial trends in all Canadian cities. The coastal cities also experience the highest trends for the warm-spell duration index (WSDI) and a decreasing trend in the cold-spell duration index (CSDI). Spatial patterns of duration indices in the Canadian coastal cities point towards hotter summers, and milder winters, whereas the cities in the Canadian prairies, the Great Lakes, and Quebec will experience hotter summers with longer durations of extremely hot weather, in addition to persistence of harsher winters.

Temperature projections have several applications, for example, in civil engineering applications, where temperature has a great role in the estimation and assessment of concrete and reinforcement deterioration. Another field of research is urban-based mortality studies, a consequence of the increasing frequency and duration of extreme temperature events. Heat-wave analysis, estimated through extreme temperature indices, forms the basis for estimating mortality rates from heat waves and other extreme temperature events.

Climate models and CMIP6 models have systematic errors in their development and hence can only predict temperature projections with a limited degree of confidence. An extension of the work in this thesis could be the use of various model performance indicators, that quantitively assess the performance of temperature projections made by CMIP6 models in Canadian cities. The future temperature projections and estimations of heat waves provide a scientific basis for a better understanding of the temperature patterns and temperature-related extreme events in Canadian cities and thus help facilitate climate change adaptation.

ACKNOWLEDGEMENTS

I would like to firstly thank my supervisor, Dr. Simon Papalexiou, whose unconditional support was instrumental in helping me achieve a dream of pursuing a Master's degree. His patience and guidance helped me overcome many obstacles in my academic journey, and I couldn’t have imagined a better supervisor for my M.Sc. degree.

I would also like to thank my co-supervisor Dr. Jian Peng, who encouraged me to pursue my passion for research through a Master's degree. I would also like to acknowledge my funding through NSERC provided by my supervisor and also my co-supervisor.

I would also like to thank Dr. Chandra Rupa Rajulapati, for her invaluable personal guidance throughout the duration of my program. Her experience in the field of research pertaining to my topic is top-notch and I feel lucky to have her mentor me throughout my program.

I would also like to thank my family and friends as their support always means a lot to me.

TABLE OF CONTENTS

LIST OF FIGURES

Chapter 1:

Chapter 2:

Appendix A:

LIST OF TABLES

Chapter 1:

Chapter 2:

Appendix A:

LIST OF ABBREVIATIONS

CDF: Cumulative Distribution Function

CMIP: Coupled model intercomparison project

DECK: Base experiments upon which CMIP models are built

ECDF: Empirical Cumulative distribution function

SCDNA: Serially complete datasets for North America

Model: Refers to a CMIP6 model

UHI: Urban heat island

SUHI: Surface urban heat-island

SSP: Shared socio-economic pathways

TX and TN: Maximum and Minimum temperature time-series

GCM: Global circulation model

RCM: Regional circulation model

TXx: Refers to value of annual/monthly maximum of TX

TNn: Refers to the annual/monthly minimum of TN

TX90p: Refers to the percentage value of TX exceeding 90^{th} percentile

TN10p: Refers to the percentage value of TN below 10^{th} percentile

WSDI: Warm spell duration index

CSDI: Cold spell duration index

ID: Icing days

FD: Frost days

Chapter 1: General Introduction

1.1 Overview

Rising temperatures have a severe impact on human health (Martin et al., 2012), food security, ecology (Piao et al., 2010), biodiversity (Urban et al., 2016), and water supply (Papalexiou et al., 2018). A predicted increase in the temperature leading to a higher frequency of heat waves and higher than average temperature across the world (Katz & Brown, 1992; Meehl & Tebaldi, 2004; Schar et al., 2004) is set to have a major effect on the ever-increasing global urban population. The increase of world urban population coincides with an ever-rising population in Canadian urban centers (Government of Canada, 2015). The increase in temperatures has severe effects on the general well-being and socio-economic aspects of human life (Gosling et al., 2009; Martin et al., 2012). Populations in the northern hemisphere are predicted to experience higher increases in temperature in the future. Several climate models actually predict that Canadian cities will experience temperatures higher than their historical average in the coming decades (Weaver, 2003). There is limited research on urban temperature projections in Canadian cities (Pengelly et al., 2007). The increase in the number of extreme temperature events in Canada could potentially affect an unprecedented number of people and communities. A projected increase of $105 - 135$ heat-stress related deaths per year over the coming decades in the city of Toronto, is an example of an impending catastrophe that could arise from a lack of preparedness (Pengelly et al., 2007)

Predicting urban temperature can be a bigger challenge than the estimation of climate parameters over larger land or ocean masses, which typically involve the use of very coarse-scale climate models. The presence of urban features, typically inherent of larger population centers across the world, creates a phenomenon known as 'Surface Urban Heat Island' (SUHI) (Gaur et al., 2018), which leads to local variations of temperature. The concept and influence of SUHI on urban temperature will not be addressed in this thesis, although the phenomenon's importance in studying urban temperature is recognized. The frequency and effect of heat waves on Canada have increased the need for accurate temperature-based urban projections to facilitate better preparation.

Given the continuous expansion of city boundaries with increasing population, the heat-island effect is always predicted to increase (Choi et al., 2014) and future urban temperature simulations to assess local temperature changes would be critical in long-term urban planning (Gallo & Xian, 2014). Hence, there is a need for a robust set of models that either encompass most of the local urban temperature variation or better represent the features of an urban environment.

Global climate models or general circulation models (GCMs) typically employs a mathematical model of the general circulation of both atmosphere and ocean processes. The Coupled model Intercomparison project (CMIP), provides a platform of tried and tested models, used extensively for temperature projections in various resolutions. This thesis involved the extraction of the CMIP6 (which is CMIP's 6^{th} iteration) ensemble of models, both historical and future, of the highest available resolution and on a daily scale, i.e., a time series with one data point per day will be used for the study. The parameters of interest of the data extracted are the Maximum temperature (TX) and Minimum temperature (TN). Various modelling groups use different sets of equations and for initial and boundary conditions leading to a set of ensemble members from each group. It is recommended to use several ensemble members to account for the unpredictability of temperature variation. Therefore, TX and TN datasets were extracted for a set of twelve models. Four different emission scenarios based on the inherent uncertainty of future temperature change (details in section 1.3 Thesis Data).

Bias is always exhibited by climate models, and CMIP6 models are no exception (Cannon et al., 2015). The bias manifests itself when a set of historical models are compared to observations. Hence, future projections of the models would need a statistical adjustment, known as bias correction. A novel bias-correction technique (section 1.4), known as Semi-parametric quantile mapping method, was used to obtain future temperature time series for four emission scenarios (see section 1.5). Bias-corrected simulations for all CMIP6 models were then analyzed for the various extreme temperature indices. Extreme temperature indices, in accordance with the Expert team of climate change detection and Indices (ETCCDI), help understand the rate of change of extreme temperature, the frequency of the change, and can also be used to analyze the spatial variation of extreme temperature across Canadian cities.

The primary objective of the thesis is to understand the transition from observed historical temperature trends to bias-corrected future trends over the variables of TX, TN and Temperature

mean (Tmean) (calculated as (TX + TN)/2), over every future emission scenario, across Canadian cities and obtain relationships between the change of the variables and the cities' populations, elevations, and respective climate zones.

Chapter-1 of the thesis focuses on an overview of the thesis topic, a succinct literature review on urban temperature, the study area, the datasets being used, and the statistical techniques that are used to correct temperature data and making reliable urban temperature projections. The Chapter is divided into the following sections: Urban temperature and study area (section 1.2), Thesis data (section 1.3), Bias correction techniques and Extreme temperature indices (section 1.4), and Thesis overview (section 1.5), which includes research questions that the thesis will aim to explore and thesis objectives, followed by individual chapter overviews.

1.2 Urban temperature and study area

1.2.1 Urban Temperature Overview

Studying the extent of urban temperature variation is a challenging task as the difference in temperature between a rural and an urban area can be as high as 7°C (Lauwaet et al., 2015). The extent of the effects of temperature varies between urban environments. Urban temperatures are complex due to altered surfaces and different land cover types leading to various thermal surfaces and high local temperature variation. Therefore, coarse-scale climate fails to account for these alterations (Wang et al., 2016). An urban temperature profile is a result of complex temperature dynamics, among other factors (Tang & Wang, 2007). The area of a city, its elevation, the land cover types, and its population are a few factors that contribute significantly to the urban heat island effect (Allen et al., 2015; Gaur et al., 2018; Wang et al., 2016). It is important to understand temperature changes for developing risk assessment strategies in urban areas. The study area hence encompasses the largest eighteen population centers in Canada.

Larger urban agglomerates contribute to higher amounts of radiative forcing. Radiative forcing is essentially the difference between the heat energy absorbed by the earth and the energy radiated back into space. This difference, which directly aids the greenhouse effect, is uncertain and hard to predict for a future time period. Hence, scenarios of climate projections are employed under various Shared Socio-economic Pathways (SSPs), each one representing a different concentration of radiative forcing. Each individual set of future projections is critical towards effective urban

planning in Canadian urban centers, and helps cope with the ever-increasing temperature and changing land cover in and around the areas of densely populated urban zones (Wicki & Parlow, 2017).

1.2.2 Study area

The largest 18 population centers in Canada are considered for the thesis. These cities have a population of over 250,000 as of the year 2020 and have also experienced some of the highest population growth since 1980. The cities are located in 7 provinces and 6 climate zones across Canada.

1.3 Thesis Data

The thesis uses two distinct sets of data; the CMIP6 data which consist of twelve models each having a historical dataset and four future datasets corresponding to future scenarios, and an observation dataset.

CMIP6, the sixth iteration of CMIP, is built on five DECK experiments (Diagnosis, Experimentation and characterization of Klima) and twenty-one Model-Intercomparison projects (MIPs), which serve as a robust means of involving a vast majority of the parameters that control climate in a region. The DECK experiments incorporated by every model in CMIP6 consist of the following simulations: Atmosphere Model Intercomparison Project (AMIP), Pre-industrial Simulations (pi-control), Historical simulations, 1% increase in CO2 atmospheric concentration (1% CO2), and four times the amount of atmospheric CO2 (4 X CO2). In the last two experiments, the change in the concentration is made for the year 1850, and then the natural climate forcings are applied until an equilibrium is attained (Eyring et al., 2016). The DECK experiments serve as the basis of all of the CMIP6 models, hence all the changes made in the individual DECK experiments (like 1% CO_2 or 4 X CO_2), are done on all the modelling groups. When applied to obtain the simulations, natural forcing (aerosols, land-use and solar variability) leads to variations and evolution within each model. One or more of the DECK experiments are tinkered with to form various variant labels or realizations in each individual model (Eyring et al., 2016). CMIP-endorsed climate models simulate meteorological and hydrological variables for more than 150 years in the past and project future changes under various scenarios assuming different radiative forcing or forcing levels called Shared Socioeconomic Pathways (SSPs).

A total of eight CMIP models, with two models having two and four subsequent realizations or variant labels (detailed in the Methods and Data section) with relatively fine resolution ($< 1°$) are selected. These have a combination of historical simulations (1979-2014) and future projections through various SSPs (2015-2100). The main SSPs, also known as Tier-1 scenarios, are the SSP1, SSP2, SSP3, and SSP5. The scenario names also have an extension based on the forcing category (Table A.1).

The CMIP6 models, are initially assessed for a given base-period (in this case 1979-2014), i.e., the historical time period. The assessment is a comparison of model data against an observation dataset. Typically, bias is estimated as the difference between the cumulative distribution function of the historical observation dataset and that of the model. The observation datasets considered were the Natural Resources Canada Meteorological Data (NRCANMET), the Watch Forcing Data (WFDEI), the Climate prediction center (CPC), and TX and TN data from the National oceanic and atmospheric administration (NOAA). All the datasets had a proportion of missing or erroneous values within the time period of 1979-2014. Station-based serially complete datasets for North America (SCDNA) for TX and TN time series for the base period (1979-2014) have been used for historical comparison with the CMIP6 models. SCDNA is based on ground observations, that have been thoroughly quality checked. The missing values were computed using a robust series of methods including quantile mapping, machine learning, and information from other reanalysis products of nearby stations. SCDNA (highlighted in Table 1.1) data are proven to perform very well when compared to other observational datasets that are notable for having a very high standing (Tang et al., 2020).

Table 1.1: List of Observation datasets considered including SCDNA data

Observation Dataset name	Institution	% of missing values
WFDEI	Hadley center for Climate Prediction and Research, Ministry of Defense, UK	4.3-5.3%
NRCANMET	National Resources Canada (NRcan)	<0.5%
CPC	National Oceanic and Atmospheric Administration (NOAA)	1%
SCDNA	Center for Hydrology, Coldwater lab, University of Saskatchewan	0%

1.4 Bias correction techniques

The assessment of climate projections requires a thorough and comprehensive method of statistical adjustment (Barrow & Sauchyn, 2017). Either one or a combination of correction techniques have to be used to assess the credibility and performance of any Global climate model, and CMIP6 models are not an exception. Hence, relatively coarser scale models like many models in CMIP6 are widely used for impact assessment studies, including the application of a correction technique since the temperature projections in an urban area as alluded to earlier are far more complicated because of the changing land use and land cover. Hence, the statistical technique of bias correction is the most common technique applied to make the temperature projections more realistic.

1.4.1 Bias-correction overview

Bias correction is a statistical adjustment made to improve the accuracy of the climate model output, but it can also be used to improve the resolution (Ehret et al., 2012). Urban Climate impact assessment using future projections will be more reliable when done with higher resolution data (Jury et al., 2015; Notaro et al., 2015). As stated earlier, coarse-scale models, would not be able to account for urban temperature variability. However, a number of models, with a reasonably high resolution, can offer an insight into temperature variation. Climate models participating in the CMIP project, are robust and offer a scientific solution to exploring and understanding urban climate variability. The gap between a coarse-scale model and urban processes can be bridged, through a statistical adjustment and bias-correction can also be used as a technique (Rummukainen, 2010), especially when mapped to a point or station observation data.

The simplest bias correction method used in temperature impact studies is the delta method. The differences (or ratios) between the simulated and observed timeseries (Graham et al., 2007; Haerter et al., 2011) are obtained and then the differences (or ratios) are added to the future timeseries (Anandhi et al., 2011). As this technique only considers the mean values, whilst other statistical parameters are ignored, the method is not conducive for effective temperature projections or impact assessment on a finer scale. Another important method, the most commonly used one, is Quantile Mapping. The main objective of this method is to use a transfer function that helps temperature simulation values of the model replicate the ones of the observation data with a great deal of accuracy (Grillakis et al., 2017), making it highly effective for several climate impact assessment studies (Grillakis et al., 2011; Ines & Hansen, 2006). Seasonal temperature over the base period is shown in Figure 1.1, where the large temperature variation across Canadian cities is presented. Bias correction is done on a monthly scale, to account for the high seasonal variation.

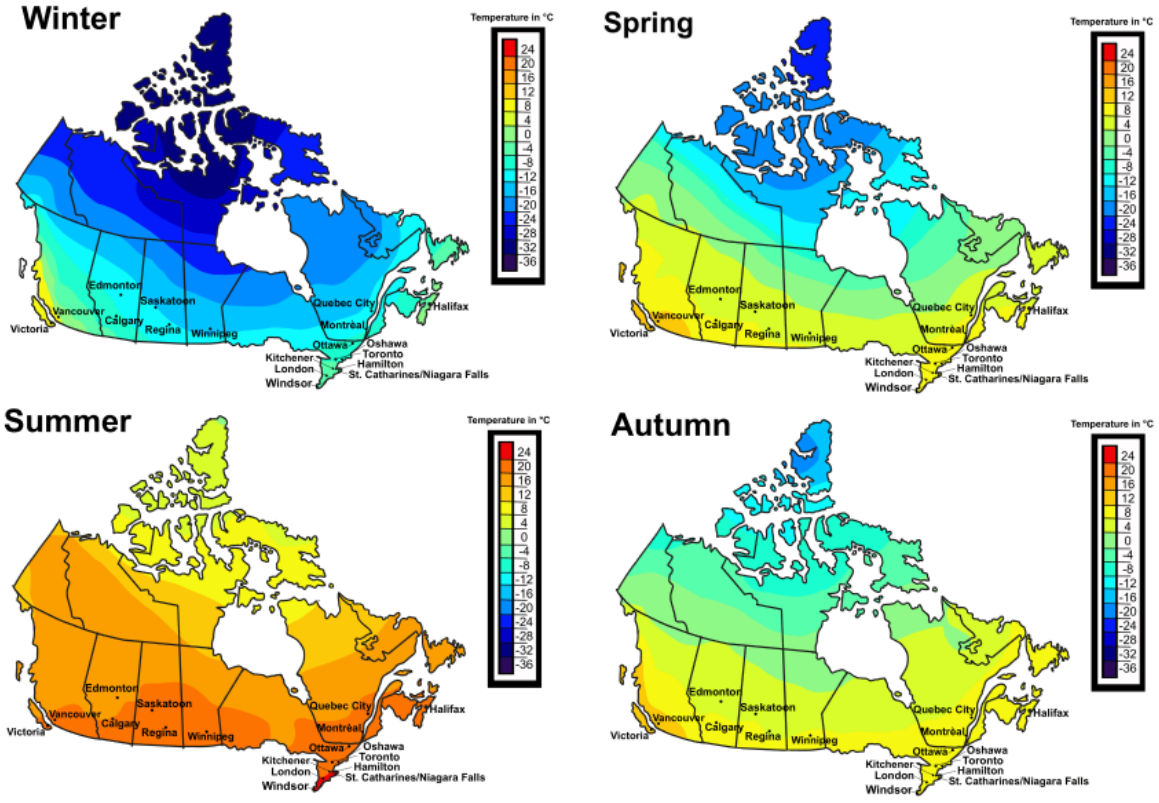

Figure 1.1: Seasonal and spatial variation of temperature across Canadian cities

The bias between an observation dataset and a modeled dataset can be visualized through a CDF plot (as shown in Figure 1.2). The CDF plot shows that there is a consistent bias across all CMIP6

models when stratified on a monthly scale.

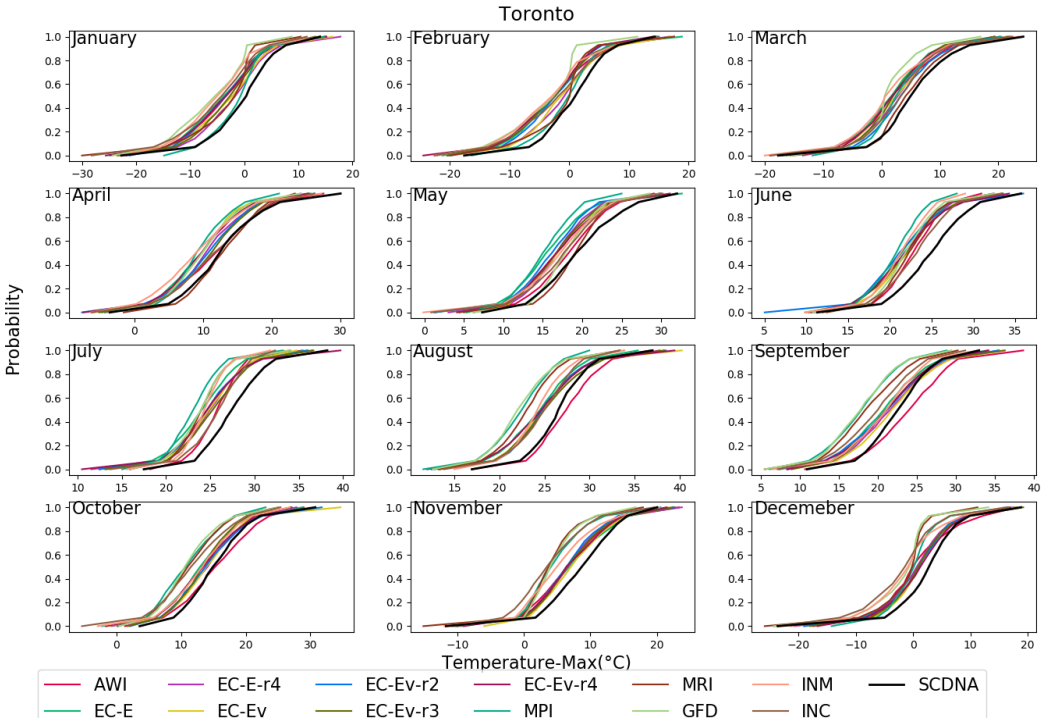

Figure 1.2: Historical (1979-2014) CDF of SCDNA data and CMIP6 modelled data, shows significant bias across all the models for one city.

1.4.2 Distribution selection

The first step of bias correction involves fitting a distribution to the data, and in most cases, the Normal distribution is usually chosen (Haerter et al., 2011; Piani et al., 2010; Terink et al., 2010). However, additional statistical distributions with more parameters have been considered for data with higher variability and skewness (Thrasher et al., 2012). Though several distributions including Normal, Johnson unbounded, and General-logistic were considered, the Skew-normal (SN) distribution (e.g., Ashour & Abdel-hameed, 2010; Azzalini, 2011) was the distribution of choice, as it captured the historical skewness of the temperature data when stratified on a monthly scale. It was estimated that three-parameter distribution (narrowed down to Skew-normal or General-logistic) had realistic fit parameters and Skew-normal distribution had the best fit (Figure 1.3)

The distribution is fit on a monthly basis as temperature is seasonal. This distribution had a good-

fit with across all cities in the study and all the CMIP6 models.

The Probability Density Function (PDF) and the Cumulative Distribution Function (CDF) of the Skew-normal (SN) distribution are given by:

$$f(x) = \frac{2}{\beta}\phi\left(\frac{x-\alpha}{\beta}\right) \times \Phi\left(\gamma\left(\frac{x-\alpha}{\beta}\right)\right) \tag{1.1}$$

$$F(x) = \Phi\left(\frac{x-\alpha}{\beta}\right) - 2\mathrm{T}\left(\left(\frac{x-\alpha}{\beta}\right), \gamma\right) \tag{1.2}$$

where $\alpha, \beta,$ and γ are location, scale and shape parameters, respectively; $\Phi(x) = (1 + \mathrm{erf}(x/\sqrt{2}))/2$ and $\phi(x) = 1/\sqrt{2\pi}\exp(-x^2/2)$ are the CDF and PDF of the standard normal distribution, and T is Owen's T function. For each city and month, the parameters are estimated by the maximum likelihood method.

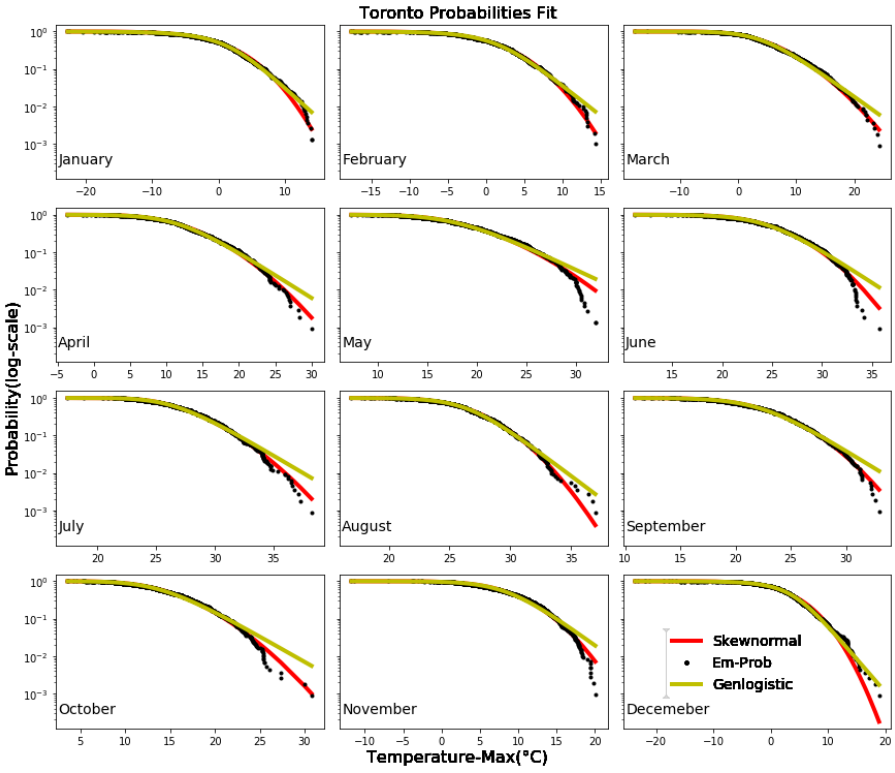

Figure 1.3: CDF plots showing the fit of probabilities of historical (SCDNA) against Skew-normal or General-logistic fitted modelled historical data.

1.4.3 Bias-correction techniques considered

The most common bias-correction methods are the traditional Quantile mapping, which makes use of a transfer function to match the cumulative distribution functions (CDF) of modelled and observed data, and the Quantile delta mapping which theoretically improves the efficiency of Quantile mapping, by calculating the delta changes at various quantiles (Chen et al., 2013; Guo et al., 2018).

Both these methods had their disadvantages; the methods either did not work very well with data that had trends or seasonality or also involved fitting at observations (historical), model (historical) and future simulations, hence having a larger margin for error.

1.4.4 Semi-parametric quantile mapping method

A novel Quantile mapping technique is used in the thesis known as the Semi-Parametric Quantile Mapping method (SPQM). The SPQM method has proven to be easier and simpler than the traditional Quantile Mapping method (QM) or the Quantile Delta Mapping (QDM), as it uses the CDF of only one set of data which is the observation historical time series.

1.4.5 Extreme temperature indices

The ETCCDI temperature indices, referred to as extreme temperature indices are based on a collaborative work put forward by the Expert team of climate change detection and Indices (ETCCDI), the World Meteorological Organization (WMO), and Climate change and predictability (CLIVAR) (Zhang et al., 2011). The indices selected in the thesis encompass all the aspects of extreme temperature assessment and are aimed to accomplish the objectives (section 1.5.1) of the thesis.

The ETCCDI temperature indices assess extreme temperature events, their frequency, and duration of occurrence over a region (Sillmann et al., 2013; Zhang et al., 2011). For example, heat waves are a consequence of extreme events, and when consecutive days are hotter than normal, this can be assessed through ETCCDI duration indices, since there are no other universally accepted standard metrics to compare heatwaves between regions, cities or time-periods (Meehl & Tebaldi, 2004; Perkins & Alexander, 2013)

The categorization of the indices will help understand the behavior of trends of temperature extremes. Each category of the indices will contribute to fulfilling an objective set out by the thesis;

the absolute indices will advance our understanding of changes in trends of TX and TN, across Canadian cities whereas the percentage indices will shed light on the frequency of trends, the duration indices on the duration, and the combination of all the indices, will help accomplish the overarching objective of understanding the behavior of future temperature extremes, and also the transition of historical to future extreme temperature trends.

Indices can also be classified based on the data used for their computation; Maximum indices, will include TXx, WSDI, TX90p, and ID, all of which are computed from the TX data, and TNn, CSDI, TN10p, and FD are computed from the TN data.

Absolute indices are calculated by considering the annual, seasonal, or monthly maximum with its units in °C, and the threshold indices are calculated as the number of days above a threshold value (in our case it is 0°C). The percentage and duration indices typically use a base period of 30 years from the 1951-2003 historical window (Alexander et al., 2006) for their computation. In this thesis a base period of 1979-2008 is used to calculate a percentile value for a 5-day moving window. The process can be described by the following steps for one day in a year:

1. For January 15^{th}, we take the days January 13^{th}, 14^{th}, 15^{th}, $16^{th,}$ and 17^{th}, for the base period, hence 150 values, and calculate the percentile value (90^{th} or 10^{th} depending on the index), over the 150 values.
2. In the future time period, the day of January 15^{th} is checked with the calculated percentile value from step 1; if the value either exceeds the 90^{th} percentile value (or is lower than the 10^{th} percentile value) it would count as a day, the percentage of the days counted in a year represent the percentage indices.
3. If the counted days from step 2 occur over at least 6 consecutive days, the annual sum of all the days is taken as the duration indices.
4. The trends are assessed and presented as change (increasing or decreasing trend) per decade for all indices. The trends are assessed using Python's Scipy library linear regression function to find the best fit line.The documentation for the Scipy library is accessed at https://docs.scipy.org/doc/scipy/reference/generated/scipy.stats.linregress.html.

1.5 Thesis Overview

1.5.1 Thesis Objectives

The thesis aims to answer the following research questions:

- How would the historical temperature trends relate to urban features and transition to future trends across the four emission scenarios?
- How are the historical and future trends of TX and TN magnitudes changing and what are the trends of frequency of occurrence of extreme events?
- What would the correlation between different spatial variations of extreme temperature indices, across future emission scenarios, and what geographical factors could be influencing these changes?

Based on these research questions, the primary objective of the thesis is to understand the changing extreme temperature trends in Canadian cities, and the following objectives help achieve the primary goal of the thesis.

- To extract and analyze TX, TN datasets through selected CMIP6 models that encompass the temperature variation exhibited in Canadian cities and make statistical adjustments by correcting bias on future projections.
- To analyze the transition of historical trends to future trends through annual Tmean trends and long-term annual Tmean trends.
- To calculate and understand the change in the magnitude, frequency, and duration of extreme temperature events in Canadian cities using selected extreme temperature indices.

1.5.2 Chapter 2 Overview

The second chapter focuses on the objectives put forward in Chapter 1 and involves extraction and analysis of TX and TN datasets for a set of eight models, two of which have four different variant labels, leading to 12 models for analysis and the SCDNA dataset, for the eighteen largest population centers, from various climate zones in Canada. Bias-corrected future projections are analyzed for extreme temperature indices. The results of the chapter will outline historical temperature trends and long-term future temperature trends. Extreme temperature changes are

assessed through eight selected ETCCDI indices or extreme temperature indices. The indices are presented and analyzed as trends (increase or decrease per decade) in two phases. The first phase, presents the indices, as boxplots, for all the CMIP6 models, for the four emission scenarios. In the second phase, the mean of the models is presented as a trend for every city on a map, to visualize spatial patterns and variation.

1.5.3 Chapter 3 Overview

Chapter 3 of the thesis includes a summary of the research findings in the previous chapters, the engineering significance of the thesis, and provides direction for future work in this research area.

References

Alexander, L. V., Zhang, X., Peterson, T. C., Caesar, J., Gleason, B., Tank, A. M. G. K., et al. (2006). Global observed changes in daily climate extremes of temperature and precipitation. *Journal of Geophysical Research: Atmospheres*, *111*(D5). https://doi.org/10.1029/2005JD006290

Allen, S. M. J., Gough, W. A., & Mohsin, T. (2015). Changes in the frequency of extreme temperature records for Toronto, Ontario, Canada. *Theoretical and Applied Climatology*, *119*(3), 481–491. https://doi.org/10.1007/s00704-014-1131-1

Anandhi, A., Frei, A., Pierson, D. C., Schneiderman, E. M., Zion, M. S., Lounsbury, D., & Matonse, A. H. (2011). Examination of change factor methodologies for climate change impact assessment. *Water Resources Research*, *47*(3). https://doi.org/10.1029/2010WR009104

Ashour, S. K., & Abdel-hameed, M. A. (2010). Approximate skew normal distribution. *Journal of Advanced Research*, *1*(4), 341–350. https://doi.org/10.1016/j.jare.2010.06.004

Azzalini, A. (2011). Skew-Normal Distribution. In M. Lovric (Ed.), *International Encyclopedia of Statistical Science* (pp. 1342–1344). Berlin, Heidelberg: Springer. https://doi.org/10.1007/978-3-642-04898-2_523

Barrow, E. M., & Sauchyn, D. J. (2017). An analysis of the performance of RCMs in simulating current climate over western Canada. *International Journal of Climatology*, *37*(S1), 640–658. https://doi.org/10.1002/joc.5028

Bastidas-Arteaga, E., Chateauneuf, A., Sánchez-Silva, M., Bressolette, Ph., & Schoefs, F. (2010). Influence of weather and global warming in chloride ingress into concrete: A stochastic

approach. *Structural Safety*, *32*(4), 238–249. https://doi.org/10.1016/j.strusafe.2010.03.002

Belda Revert, A., De Weerdt, K., Hornbostel, K., & Geiker, M. R. (2018). Carbonation-induced corrosion: Investigation of the corrosion onset. *Construction and Building Materials*, *162*, 847–856. https://doi.org/10.1016/j.conbuildmat.2017.12.066

Bonsal, B. R., Zhang, X., Vincent, L. A., & Hogg, W. D. (2001). Characteristics of Daily and Extreme Temperatures over Canada. *Journal of Climate*, *14*(9), 1959–1976. https://doi.org/10.1175/1520-0442(2001)014<1959:CODAET>2.0.CO;2

Buishand, T. A., & Brandsma, T. (1999). Dependence of precipitation on temperature at Florence and Livorno (Italy). *Climate Research*, *12*(1), 53–63. Retrieved from http://www.jstor.org/stable/24865998

Bush,E & Flato,G. (2019). *Canada's Changing Climate Report*. Natural Resources Canada. Retrieved from https://www.nrcan.gc.ca/climate-change/impacts-adaptations/canadas-changing-climate-report/21177

Cannon, A. J., Sobie, S. R., & Murdock, T. Q. (2015). Bias Correction of GCM Precipitation by Quantile Mapping: How Well Do Methods Preserve Changes in Quantiles and Extremes? *Journal of Climate*, *28*(17), 6938–6959. https://doi.org/10.1175/JCLI-D-14-00754.1

Chen, J., Brissette, F. P., Chaumont, D., & Braun, M. (2013). Finding appropriate bias correction methods in downscaling precipitation for hydrologic impact studies over North America. *Water Resources Research*, *49*(7), 4187–4205. https://doi.org/10.1002/wrcr.20331

Choi, Y.-Y., Suh, M.-S., & Park, K.-H. (2014). Assessment of Surface Urban Heat Islands over Three Megacities in East Asia Using Land Surface Temperature Data Retrieved from

COMS. *Remote Sensing*, *6*(6), 5852–5867. https://doi.org/10.3390/rs6065852

Daniel, M., Lemonsu, A., Déqué, M., Somot, S., Alias, A., & Masson, V. (2019). Benefits of explicit urban parameterization in regional climate modeling to study climate and city interactions. *Climate Dynamics*, *52*(5), 2745–2764. https://doi.org/10.1007/s00382-018-4289-x

Dave Sauchyn & Debra Davidson. (2020). *Canada in a Changing Climate: Regional Perspectives Report* (p. 72).

Diffenbaugh, N. S., & Giorgi, F. (2012). Climate change hotspots in the CMIP5 global climate model ensemble. *Climatic Change*, *114*(3), 813–822. https://doi.org/10.1007/s10584-012-0570-x

Ehret, U., Zehe, E., Wulfmeyer, V., Warrach-Sagi, K., & Liebert, J. (2012). HESS Opinions "Should we apply bias correction to global and regional climate model data?" *Hydrology and Earth System Sciences*, *16*(9), 3391–3404. https://doi.org/10.5194/hess-16-3391-2012

Eyring, V., Bony, S., Meehl, G. A., Senior, C. A., Stevens, B., Stouffer, R. J., & Taylor, K. E. (2016). Overview of the Coupled Model Intercomparison Project Phase 6 (CMIP6) experimental design and organization. *Geoscientific Model Development*, *9*(5), 1937–1958. https://doi.org/10.5194/gmd-9-1937-2016

Fortune, M. K., Mustard, C. A., Etches, J. J. C., & Chambers, A. G. (2013). Work-attributed Illness Arising From Excess Heat Exposure in Ontario, 2004–2010. *Canadian Journal of Public Health*, *104*(5), e420–e426. https://doi.org/10.17269/cjph.104.3984

Gallo, K., & Xian, G. (2014). Application of spatially gridded temperature and land cover data sets for urban heat island analysis. *Urban Climate*, *8*, 1–10.

https://doi.org/10.1016/j.uclim.2014.04.005

Gaur, A., Eichenbaum, M. K., & Simonovic, S. P. (2018). Analysis and modelling of surface Urban Heat Island in 20 Canadian cities under climate and land-cover change. *Journal of Environmental Management*, *206*, 145–157. https://doi.org/10.1016/j.jenvman.2017.10.002

Gosling, S. N., Lowe, J. A., McGregor, G. R., Pelling, M., & Malamud, B. D. (2009). Associations between elevated atmospheric temperature and human mortality: a critical review of the literature. *Climatic Change*, *92*(3), 299–341. https://doi.org/10.1007/s10584-008-9441-x

Government of Canada, S. C. (2015, April 13). Canada goes urban. Retrieved April 13, 2020, from https://www150.statcan.gc.ca/n1/pub/11-630-x/11-630-x2015004-eng.htm

Graham, L. P., Andréasson, J., & Carlsson, B. (2007). Assessing climate change impacts on hydrology from an ensemble of regional climate models, model scales and linking methods – a case study on the Lule River basin. *Climatic Change*, *81*(1), 293–307. https://doi.org/10.1007/s10584-006-9215-2

Grillakis, M. G., Koutroulis, A. G., & Tsanis, I. K. (2011). Climate change impact on the hydrology of Spencer Creek watershed in Southern Ontario, Canada. *Journal of Hydrology*, *409*(1), 1–19. https://doi.org/10.1016/j.jhydrol.2011.06.018

Grillakis, M. G., Koutroulis, A. G., Daliakopoulos, I. N., Tsanis, I. K., & Tsanis, I. K. (2017). A method to preserve trends in quantile mapping bias correction of climate modeled temperature. *Earth System Dynamics*, *8*, 889–900. https://doi.org/10.5194/esd-8-889-2017

Guo, L.-Y., Gao, Q., Jiang, Z.-H., & Li, L. (2018). Bias correction and projection of surface air temperature in LMDZ multiple simulation over central and eastern China. *Advances in*

Climate Change Research, *9*(1), 81–92. https://doi.org/10.1016/j.accre.2018.02.003

Haerter, J. O., Hagemann, S., Moseley, C., & Piani, C. (2011). Climate model bias correction and the role of timescales. *Hydrology and Earth System Sciences*, *15*(3), 1065–1079. https://doi.org/10.5194/hess-15-1065-2011

Ines, A. V. M., & Hansen, J. W. (2006). Bias correction of daily GCM rainfall for crop simulation studies. *Agricultural and Forest Meteorology*, *138*(1), 44–53. https://doi.org/10.1016/j.agrformet.2006.03.009

Jury, M. W., Prein, A. F., Truhetz, H., & Gobiet, A. (2015). Evaluation of CMIP5 Models in the Context of Dynamical Downscaling over Europe. *Journal of Climate*, *28*(14), 5575–5582. https://doi.org/10.1175/JCLI-D-14-00430.1

Katz, R. W., & Brown, B. G. (1992). Extreme events in a changing climate: Variability is more important than averages. *Climatic Change*, *21*(3), 289–302. https://doi.org/10.1007/BF00139728

Keatinge, W. R., & Donaldson, G. C. (2004, November). The impact of global warming on health and mortality. *Southern Medical Journal*, *97*(11), 1093+. Retrieved from http://link.gale.com/apps/doc/A126076453/EAIM?sid=bookmark-EAIM&xid=2396cc48

Knutti, R., & Sedláček, J. (2013). Robustness and uncertainties in the new CMIP5 climate model projections. *Nature Climate Change*, *3*(4), 369–373. https://doi.org/10.1038/nclimate1716

Kolb, S., Radon, K., Valois, M.-F., Héguy, L., & Goldberg, M. S. (2007). The Short-Term Influence of Weather on Daily Mortality in Congestive Heart Failure. *Archives of Environmental & Occupational Health*, *62*(4), 169–176. https://doi.org/10.3200/AEOH.62.4.169-176

Lauwaet, D., Hooyberghs, H., Maiheu, B., Lefebvre, W., Driesen, G., Looy, S. V., & Ridder, K. D. (2015). Detailed Urban Heat Island Projections for Cities Worldwide: Dynamical Downscaling CMIP5 Global Climate Models. *Climate*, *3*(2), 391–415. https://doi.org/10.3390/cli3020391

Li, H., Sheffield, J., & Wood, E. F. (2010). Bias correction of monthly precipitation and temperature fields from Intergovernmental Panel on Climate Change AR4 models using equidistant quantile matching. *Journal of Geophysical Research: Atmospheres*, *115*(D10). https://doi.org/10.1029/2009JD012882

Li, Z., Huang, G., Huang, W., Lin, Q., Liao, R., & Fan, Y. (2018). Future changes of temperature and heat waves in Ontario, Canada. *Theoretical and Applied Climatology*, *132*(3), 1029–1038. https://doi.org/10.1007/s00704-017-2123-8

LUO, N., GUO, Y., GAO, Z., CHEN, K., & CHOU, J. (2020). Assessment of CMIP6 and CMIP5 model performance for extreme temperature in China. *Atmospheric and Oceanic Science Letters*, *13*(6), 589–597. https://doi.org/10.1080/16742834.2020.1808430

Martin, S. L., Cakmak, S., Hebbern, C. A., Avramescu, M.-L., & Tremblay, N. (2012). Climate change and future temperature-related mortality in 15 Canadian cities. *International Journal of Biometeorology*, *56*(4), 605–619. https://doi.org/10.1007/s00484-011-0449-y

Maurer, E. P., Brekke, L., Pruitt, T., & Duffy, P. B. (2007). Fine-resolution climate projections enhance regional climate change impact studies. *Eos, Transactions American Geophysical Union*, *88*(47), 504–504. https://doi.org/10.1029/2007EO470006

McMichael, A. J., Woodruff, R. E., & Hales, S. (2006). Climate change and human health: present and future risks. *The Lancet*, *367*(9513), 859–869. https://doi.org/10.1016/S0140-

6736(06)68079-3

Meehl, G. A., & Tebaldi, C. (2004). More Intense, More Frequent, and Longer Lasting Heat Waves in the 21st Century. *Science*, *305*(5686), 994–997. Retrieved from https://www.jstor.org/stable/3837565

Murray, V., & Ebi, K. L. (2012). IPCC Special Report on Managing the Risks of Extreme Events and Disasters to Advance Climate Change Adaptation (SREX). *Journal of Epidemiology and Community Health (1979-)*, *66*(9), 759–760. Retrieved from http://www.jstor.org/stable/23269103

Notaro, M., Bennington, V., & Lofgren, B. (2015). Dynamical Downscaling-Based Projections of Great Lakes Water Levels*+. *Journal of Climate*, *28*(24), 9721–9745. https://doi.org/10.1175/JCLI-D-14-00847.1

Papalexiou, S. M., AghaKouchak, A., Trenberth, K. E., & Foufoula-Georgiou, E. (2018). Global, Regional, and Megacity Trends in the Highest Temperature of the Year: Diagnostics and Evidence for Accelerating Trends. *Earth's Future*, *6*(1), 71–79. https://doi.org/10.1002/2017EF000709

Peacock, S. (2012). Projected Twenty-First-Century Changes in Temperature, Precipitation, and Snow Cover over North America in CCSM4. *Journal of Climate*, *25*(13), 4405–4429. https://doi.org/10.1175/JCLI-D-11-00214.1

Pengelly, L. D., Campbell, M. E., Cheng, C. S., Fu, C., Gingrich, S. E., & Macfarlane, R. (2007). Anatomy of Heat Waves and Mortality in Toronto. *Canadian Journal of Public Health*, *98*(5), 364–368. https://doi.org/10.1007/BF03405420

Perkins, S. E., & Alexander, L. V. (2013). On the Measurement of Heat Waves. *Journal of Climate*,

26(13), 4500–4517. https://doi.org/10.1175/JCLI-D-12-00383.1

Piani, C., Weedon, G. P., Best, M., Gomes, S. M., Viterbo, P., Hagemann, S., & Haerter, J. O. (2010). Statistical bias correction of global simulated daily precipitation and temperature for the application of hydrological models. *Journal of Hydrology*, *395*(3), 199–215. https://doi.org/10.1016/j.jhydrol.2010.10.024

Piao, S., Ciais, P., Huang, Y., Shen, Z., Peng, S., Li, J., et al. (2010). The impacts of climate change on water resources and agriculture in China. *Nature*, *467*(7311), 43–51. https://doi.org/10.1038/nature09364

Plummer, D. A., Caya, D., Frigon, A., Côté, H., Giguère, M., Paquin, D., et al. (2006). Climate and Climate Change over North America as Simulated by the Canadian RCM. *Journal of Climate*, *19*(13), 3112–3132. https://doi.org/10.1175/JCLI3769.1

Power, S., Delage, F., Wang, G., Smith, I., & Kociuba, G. (2017). Apparent limitations in the ability of CMIP5 climate models to simulate recent multi-decadal change in surface temperature: implications for global temperature projections. *Climate Dynamics*, *49*(1), 53–69. https://doi.org/10.1007/s00382-016-3326-x

Reichstein, M., Bahn, M., Ciais, P., Frank, D., Mahecha, M. D., Seneviratne, S. I., et al. (2013). Climate extremes and the carbon cycle. *Nature*, *500*(7462), 287–295. https://doi.org/10.1038/nature12350

Rizwan, A. M., Dennis, L. Y. C., & Liu, C. (2008). A review on the generation, determination and mitigation of Urban Heat Island. *Journal of Environmental Sciences*, *20*(1), 120–128. https://doi.org/10.1016/S1001-0742(08)60019-4

Rummukainen, M. (2010). State-of-the-art with regional climate models. *WIREs Climate Change*,

1(1), 82–96. https://doi.org/10.1002/wcc.8

Schar, C., Vidale, P. L., Luthi, D., Frei, C., Haberli, C., Liniger, M. A., & Appenzeller, C. (2004). The role of increasing temperature variability in European summer heatwaves. *Nature*, *427*(6972), 332-. Retrieved from http://link.gale.com/apps/doc/A186371710/EAIM?u=usaskmain&sid=zotero&xid=e5e58c2c

Seneviratne, S. I., Donat, M. G., Pitman, A. J., Knutti, R., & Wilby, R. L. (2016). Allowable CO 2 emissions based on regional and impact-related climate targets. *Nature*, *529*(7587), 477–483. https://doi.org/10.1038/nature16542

Sillmann, J., Kharin, V. V., Zhang, X., Zwiers, F. W., & Bronaugh, D. (2013). Climate extremes indices in the CMIP5 multimodel ensemble: Part 1. Model evaluation in the present climate. *Journal of Geophysical Research: Atmospheres*, *118*(4), 1716–1733. https://doi.org/10.1002/jgrd.50203

Sillmann, J., Kharin, V. V., Zwiers, F. W., Zhang, X., & Bronaugh, D. (2013). Climate extremes indices in the CMIP5 multimodel ensemble: Part 2. Future climate projections. *Journal of Geophysical Research: Atmospheres*, *118*(6), 2473–2493. https://doi.org/10.1002/jgrd.50188

Silva, A., Neves, R., & de Brito, J. (2014). Statistical modelling of carbonation in reinforced concrete. *Cement and Concrete Composites*, *50*, 73–81. https://doi.org/10.1016/j.cemconcomp.2013.12.001

Smoyer-Tomic, K. E., & Rainham, D. G. C. (2001). Beating the heat: development and evaluation of a Canadian hot weather health-response plan. (Articles). *Environmental Health*

Perspectives, *109*(12), 1241-. Retrieved from http://link.gale.com/apps/doc/A82551832/EAIM?u=usaskmain&sid=zotero&xid=959742ab

Stewart, M. G., Wang, X., & Nguyen, M. N. (2011). Climate change impact and risks of concrete infrastructure deterioration. *Engineering Structures*, *33*(4), 1326–1337. https://doi.org/10.1016/j.engstruct.2011.01.010

Tang, G., Clark, M. P., Newman, A. J., Wood, A. W., Papalexiou, S. M., Vionnet, V., & Whitfield, P. H. (2020). SCDNA: a serially complete precipitation and temperature dataset for North America from 1979 to 2018. *Earth System Science Data*, *12*(4), 2381–2409. https://doi.org/10.5194/essd-12-2381-2020

Tang, U. W., & Wang, Z. S. (2007). Influences of urban forms on traffic-induced noise and air pollution: Results from a modelling system. *Environmental Modelling & Software*, *22*(12), 1750–1764. https://doi.org/10.1016/j.envsoft.2007.02.003

Tebaldi, C., & Knutti, R. (2007). The use of the multi-model ensemble in probabilistic climate projections. *Philosophical Transactions of the Royal Society A: Mathematical, Physical and Engineering Sciences*, *365*(1857), 2053–2075. https://doi.org/10.1098/rsta.2007.2076

Terink, W., Hurkmans, R. T. W. L., Torfs, P. J. J. F., & Uijlenhoet, R. (2010). Evaluation of a bias correction method applied to downscaled precipitation and temperature reanalysis for the Rhine basin. *Hydrology and Earth System Sciences*, *14*(4), 687–703. https://doi.org/10.5194/hess-14-687-2010

Teutschbein, C., & Seibert, J. (2012). Bias correction of regional climate model simulations for hydrological climate-change impact studies: Review and evaluation of different methods.

Journal of Hydrology, *456–457*, 12–29. https://doi.org/10.1016/j.jhydrol.2012.05.052

Thrasher, B., Maurer, E. P., McKellar, C., & Duffy, P. B. (2012). Technical Note: Bias correcting climate model simulated daily temperature extremes with quantile mapping. *Hydrology and Earth System Sciences*, *16*(9), 3309. Retrieved from http://link.gale.com/apps/doc/A481466919/EAIM?u=usaskmain&sid=zotero&xid=93e37ec8

Urban, M. C., Bocedi, G., Hendry, A. P., Mihoub, J.-B., Pe'er, G., Singer, A., et al. (2016). Improving the forecast for biodiversity under climate change. *Science*, *353*(6304). https://doi.org/10.1126/science.aad8466

Wang, J., Zhan, Q., & Guo, H. (2016). The Morphology, Dynamics and Potential Hotspots of Land Surface Temperature at a Local Scale in Urban Areas. *Remote Sensing*, *8*(1), 18. https://doi.org/10.3390/rs8010018

Weaver, A. J. (2003). The Science of Climate Change. *Geoscience Canada*. Retrieved from https://journals.lib.unb.ca/index.php/GC/article/view/4147

Wicki, A., & Parlow, E. (2017). Multiple Regression Analysis for Unmixing of Surface Temperature Data in an Urban Environment. *Remote Sensing*, *9*(7), 684. https://doi.org/10.3390/rs9070684

Zhang, X., Alexander, L., Hegerl, G. C., Jones, P., Tank, A. K., Peterson, T. C., et al. (2011). Indices for monitoring changes in extremes based on daily temperature and precipitation data. *WIREs Climate Change*, *2*(6), 851–870. https://doi.org/10.1002/wcc.147

Zhou, X., Huang, G., Wang, X., Fan, Y., & Cheng, G. (2018). A coupled dynamical-copula downscaling approach for temperature projections over the Canadian Prairies. *Climate*

Dynamics, *51*(7), 2413–2431. https://doi.org/10.1007/s00382-017-4020-3

Chapter-2: Analysis of extreme temperature changes using ETCCDI indices and CMIP6 data in Canadian cities

Abstract

This study incorporates the selected ETCCDI indices to assess changes in temperature extremes in the largest 18 Canadian cities. Bias-corrected maximum and minimum temperature projections of eight CMIP6 models using four Shared Socio-economic Pathways (SSPs) were used to calculate the extreme temperature indices. The indices, grouped as absolute, duration, threshold, and percentile indices, offered varying spatial and magnitude variation amongst the cities involved in the study. The increase of absolute indices is uneven throughout the 21st century, although other indices have an evenly increasing or decreasing trend, based on the city. Absolute indices predicted the highest increasing trends in the cities in the Prairies climate zone over the last three decades of the 21st century (2071-2100), whereas the duration and the threshold indices are predicted to have the highest trends in coastal Canadian cities. Despite increasing trends in magnitudes of minimum and maximum temperature extremes, it is projected that the duration and frequency of lower temperature extremes will persist, especially in the cities in the Canadian prairies and the Great Lakes climate zones. The results of this study will aid in further understanding extreme temperature-related phenomena like heat waves and will assist in urban planning and mitigation strategies.

2.1 Introduction

About 55% of the world's population lives in urban areas and this proportion is expected to rise to 66% by 2050 (United Nations et al., 2019). In Canada, over 80% of the population lives in urban areas currently, with a steep decline in the rural population from 84% in 1851 to 18.9% as of 2011 (Government of Canada, 2015). Due to the ever-growing population and a dense network of heavy construction/buildings within a constrained space, urban areas typically have a different climate

with increased temperatures compared to their surrounding rural areas, creating a 'heat island' (Gaur et al., 2018). This has a severe effect on the environment, from reduced air quality to structural deterioration of concrete infrastructure (Lauwaet et al., 2015; Stewart et al., 2011), general well-being, and socio-economic aspects of human life (Gosling et al., 2009; Martin et al., 2012). In addition, temperature changes have a severe effect on precipitation patterns, frequency, and duration (Buishand & Brandsma, 1999). There is a predicted increase in temperature variation leading to a higher frequency of heat waves across the world (Katz & Brown, 1992; Meehl & Tebaldi, 2004; Schar et al., 2004). The threatening effects of heat waves in several parts of the globe have increased the importance of temperature-based projections to facilitate better risk management and disaster preparedness (Martin et al., 2012). Therefore, it is of paramount importance to understand historical and future temperature changes in urban areas for risk analysis and adaptation and mitigation measures development.

North temperate and polar regions are expected to experience higher increases in temperature compared to the tropics in the future. Previous versions of climate models predict that Canadian cities will experience temperatures higher than their averages in the coming decades (Weaver, 2003). Canada has fewer studies conducted on the extent of heat waves in the last few decades, when compared to other countries (Pengelly et al., 2007). In the city of Toronto, heat waves are responsible for 120 deaths per year and this number is expected to rise to $144 - 447$, as the number of extreme hot-weather periods is predicted to be more frequent in the coming decades, both in Toronto and the nearby urban centers in Ontario (Allen et al., 2015). The frequency and effect of heat waves on Canada have increased the need for accurate temperature-based projections to facilitate better preparation. The likelihood of temperature extremes is always on the rise, even though it is hard to determine if the sole reason for this increase is the greenhouse emissions. However, the greenhouse emissions trend in the last century, point towards a rise in extreme events such as heat waves, whereas the likelihood of extreme frost events has decreased (Murray & Ebi, 2012). Hence, statistical studies on extreme events, help with mitigation strategies to limit extreme damage that can occur from extreme events (Reichstein et al., 2013). Given the continuous expansion of city boundaries with increasing population, future climate simulations are critical for long-term urban planning (Gallo & Xian, 2014).

Previous versions of CMIP simulations have been extensively used and thoroughly analyzed for

both historical and future periods—historical for quantifying the simulations' accuracy, and future for understanding the projected change (Barrow & Sauchyn, 2017; Gaur et al., 2018; Lauwaet et al., 2015). The majority of CMIP models from the previous versions of CMIP, predict a global temperature increase (Diffenbaugh & Giorgi, 2012). Although CMIP models overall do not fully represent the local features of urban areas (Knutti & Sedláček, 2013; Tebaldi & Knutti, 2007), CMIP6-endorsed models are advantageous due to the fact that they are modelled using different initial conditions for historical climate and four major scenarios for future projections leading to an ensemble of simulations. CMIP data are also available for longer time scales (~ 150 years for historical simulations and till 2100 for future projections) enabling us to better understand changes in temperature.

A compendious way of assessing climate projections does require a thorough and comprehensive method of analysis (Barrow & Sauchyn, 2017). Either one or a combination of correction techniques must be used to assess the credibility and performance of CMIP6 models. Bias correction is a statistical adjustment made to improve the accuracy of the model output (Ehret et al., 2012). It corrects the CMIP models' inability to capture features that would contribute to temperature variation in urban areas. Urban climate impact assessments using future projections will be more reliant when done with higher resolution data (Jury et al., 2015; Notaro et al., 2015). Bias correction methods range from simple delta mapping methods to many types of Quantile mapping methods (Graham et al., 2007; Grillakis et al., 2011; Haerter et al., 2011; Ines & Hansen, 2006). The normal distribution is usually considered as the distribution of the model data. (Haerter et al., 2011; Piani et al., 2010; Terink et al., 2010). However, additional statistical distributions with higher parameters will need to be considered, for data comprised of higher variability and skewness (Thrasher et al., 2012).

Bias correction and downscaling techniques are essential to make meaningful projections of climate indices (Maurer et al., 2007). Studying temperature extremes often consists of studying the 16 temperature-related extremes indices. The temperature indices are developed through the collaborative work of the Expert team of climate change detection and Indices (ETCCDI), the World Meteorological Organization (WMO), and the Climate change and predictability (CLIVAR) (Alexander et al., 2006). Temperature indices effectively capture the varying climate of a region or a country with emphasis on temperature duration, intensity, and frequency, making them highly effective for validating the changing climate of a region (Zhang et al., 2011).

2.2 Methodology and study area

2.2.1 Study area

The study incorporates the top eighteen cities with the highest population (Table 2.1). Geographically, the cities lie in various climate zones of Canada (Plummer et al., 2006) (Figure 2.1). Toronto, Hamilton, London, Ottawa-Gatineau, St. Catharines-Niagara Falls, Windsor, Kitchener, and Oshawa are large urban centers in Ontario and Quebec, surrounded by the Great Lakes and in the St Lawrence climactic zone. Cities in the province of Quebec, Montreal and Quebec City, lie in the Northeastern Forest zone, a climactic zone affected by Arctic tundra, the Atlantic Ocean and the Great Lakes. Winnipeg, Saskatoon and Regina are the cities in the Canadian prairies, characterized by long winters and short summers with longer sunshine hours. Vancouver and Victoria are situated in the Pacific climate zone in western Canada, and have relatively milder winters and higher amount of precipitation compared to other regions. Halifax is on the eastern end, in the Atlantic climate zone, where climate is heavily regulated by winds generated by Atlantic Ocean currents. Calgary and Edmonton are located at the periphery of the Canadian prairies and the Northwestern Forest and hence are impacted by climactic conditions of both zones. These climate zones, play a vital role in understanding the spatial variation of temperature in both the historical and the future contexts.

Table 2.1: List of Canada's highest population centers, along with area, elevation and population.

City Name	Population (2020 Consensus)	Province	Area(km²)	Elevation(m)
Toronto	6,255,000	ON	7124	85
Montreal	4,247,000	Que	4258	40
Vancouver	2,606,000	BC	2700	31
Calgary	1,581,000	ALB	825	1050
Edmonton	1,491,000	ALB	684	645
Ottawa-Gatineau	1,408,000	ON	2790	70
Winnipeg	825,000	MB	464	239
Quebec City	832,000	Que	484	98
Hamilton	771,000	ON	1138	324
Kitchener	571,000	ON	136.9	301
London	511,000	ON	1572	251
Victoria	390,000	BC	19.47	23
Halifax	415,000	NS	234.72	102
Oshawa	402,000	ON	145.7	106
Windsor	338,000	ON	146.3	190
St. Catharines-Niagara Falls	416,000	ON	302.81	98
Saskatoon	331,000	SK	228.1	482
Regina	263,184	SK	180	577

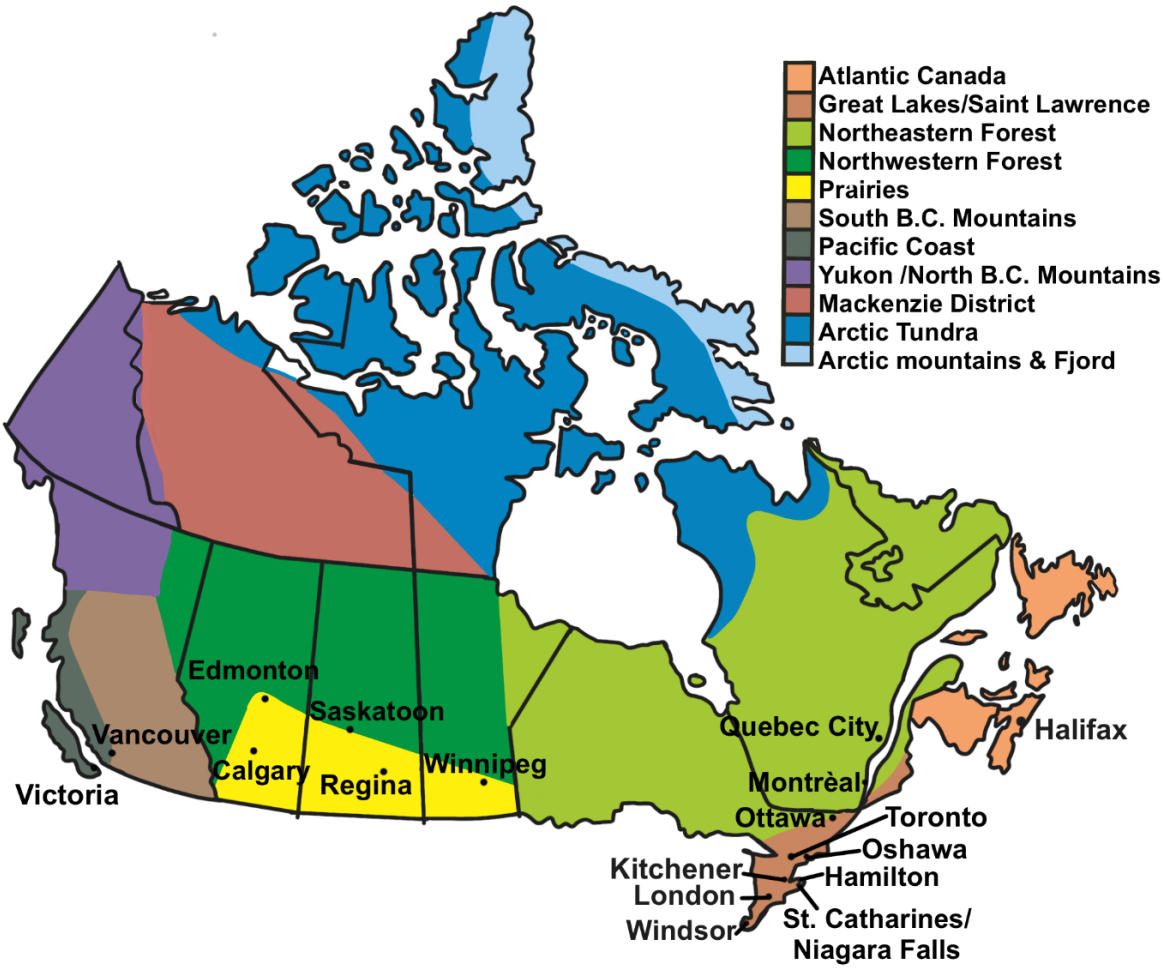

Figure 2.1: Cities used in the analysis are situated in 6 climate zones and 7 provinces across most populated regions of Canada.

2.2.2 Data

Simulated historical daily maximum and minimum temperature values (TX and TN) outputs of 8 CMIP6 models were retrieved from the Earth System Grid Federation (https://esgf-node.llnl.gov/projects/esgf-llnl/). Although more than 40 CMIP6 models are available, models with fine resolution, that is, less than 1° on either direction, are chosen (Table 2.2). Four scenarios for future, that is, SSP1-2.6, SSP2-4.5, SSP3-7.0 and SSP5-8.5, are considered. Simulations with same variant label that are available for the historical and all four SSPs are considered (Table A.1). Serially Complete Dataset for North America (SCDNA), a database for North America considering station observations is used in this work. The data were thoroughly quality checked and missing values are imputed using a robust series of methods including quantile mapping, machine learning

and information from other reanalysis products of nearby stations (Tang et al., 2020). Stations that are closest to the city latitude-longitude are chosen. TX and TN timeseries for 1979-2014 period is considered here.

Table 2.2: Eight CMIP6 models) with resolution of 1° or lower, that are used in the analysis of the thesis, along with a station-based observation dataset.

Model Name	Institution	Model Identifier	No of grids (Lat X Lon)
AWI-CM-1-1-MR	Alfred Wegener Institute, Helmholtz center for Polar and Marine Research, Germany	AWI	192 × 384
EC-Earth3	Consortium of various institutions from Spain, Italy, Denmark, Finland, Germany, Ireland, Portugal, Netherlands, Norway, UK, Belgium, and Sweden	EC-E or EC-E-r4	256 × 512
EC-Earth3-Veg	Consortium of various institutions from Spain, Italy, Denmark, Finland, Germany, Ireland, Portugal, Netherlands, Norway, UK, Belgium, and Sweden	EC-Ev or EC-Ev-r2, EC-Ev-r3, EC-Ev-r4	256 × 512
GFDL-ESM4	National Oceanic and Atmospheric Administration, GFDL, Princeton, USA	GFD	180 × 288
GFDL-CM4	National Oceanic and Atmospheric Administration, GFDL, Princeton, USA	GFL	180 × 288
INM-CM4-8	Institute for Numerical Mathematics, Russian Academy of Science, Moscow, Russia	INC	120 × 180
INM-CM5-0	Institute for Numerical Mathematics, Russian Academy of Science, Moscow, Russia	INM	120 × 180
MPI-ESM1-2-HR	Max Planck Institute for Meteorology	MPE	192 × 384

MRI-ESM2-0	Meteorological Research Institute, Tsukuba, Japan	MRI	160 × 320
SCDNA	Global Water Futures, Univ. of Saskatchewan	SCD	Station

2.2.3 Methods

Quantile Mapping (QM), a method of bias correction technique, can preserve the statistical properties of observation data at all quantiles and is better than other commonly used methods (e.g. delta method) of bias correction (Chen et al., 2013; Teutschbein & Seibert, 2012). Some extended methods, such as the Detrended QM (DQM) and the Quantile Delta Mapping (QDM) are used to include varying biases such as non-stationary biases in the projected timeseries (Cannon et al., 2015; H. Li et al., 2010). While in the DQM the trend in long-term mean is removed prior to quantile mapping, in the QDM relative changes between historical and future simulations are preserved at all quantiles instead of just the mean as in detrended QM. Both these methods require fitting probability distribution at three levels if a parametric case is considered.

While non-parametric methods avoid the uncertainties due to the fitting, the bias-corrected projections are highly dependent on the quality of data that would be mapped, which are observation data. A Semi-Parametric Quantile Mapping (SPQM) method is employed in this work. Here we fit a skew-normal ($\mathcal{SN}$) distribution to the observed data and empirical quantiles are used for future simulations. $\mathcal{SN}$ distribution (e.g., Ashour & Abdel-hameed, 2010; Azzalini, 2011) is used as the observational data exhibits a minor skewness in both directions (positive or negative skewness). To account for seasonality, the distribution is fit on a monthly basis. Though we have tried fitting Log-normal and Johnson unbounded, the skew-normal is found to be the best fit. The PDF and CDF of the $\mathcal{SN}$ distribution are given by

$$f(x) = \frac{2}{\beta}\phi\left(\frac{x-\alpha}{\beta}\right) \times \Phi\left(\gamma\left(\frac{x-\alpha}{\beta}\right)\right) \tag{2.1}$$

$$F(x) = \Phi\left(\frac{x-\alpha}{\beta}\right) - 2\mathrm{T}\left(\left(\frac{x-\alpha}{\beta}\right), \gamma\right) \tag{2.2}$$

where $\alpha, \beta,$ and γ are location, sale and shape parameters, respectively; $\Phi(x) = (1 +$

$\mathrm{erf}(x/\sqrt{2}))/2$ and $\phi(x) = 1/\sqrt{2\pi}\exp(-x^2/2)$ are the cdf and pdf of the standard normal distribution, and T is Owen's T function. For each city and month, the parameters are estimated by the maximum likelihood method. For a given month (m), the quantile mapped future projections $\hat{x}_{\mathrm{fs},m}(t)$ using SPQM is given by:

$$\hat{x}_{\mathrm{fs},m}(t) = F_{o,m}\left(q_{\mathrm{fs},m}(t)\right) \tag{2.3}$$

where $q_{\mathrm{fs},m}(t)$ is the empirical probability of future simulation, $x_{\mathrm{fs},m}(t)$. The empirical probabilities for future simulations are obtained using the Weibull plotting position formula ($(r/(N+1))$, where r is the rank of a datapoint of interest and N is the total sample size. As a linear trend is noted in the projections, specifically for higher SSPs (SSP 5-85 and SSP 3-70), the timeseries is detrended first and SPQM is applied.

The steps of the SPQM method are

1. $\mathcal{SN}$ distribution is fit to historical observations in a monthly basis.
2. for a given model, variant label, and SSP, the projected timeseries is detrended
3. on the detrended timeseries, the empirical probabilities using the Weibull plotting position are calculated
4. using CDF of $\mathcal{SN}$ distribution on the empirical probabilities, projected temperature for each month is calculated
5. finally, the trend, which was removed in step 2, was added back to obtain the quantile mapped future projections.

The mean temperature timeseries is obtained for both historical observations and bias-corrected projections. First, the historical temperature trends are calculated for the annual mean timeseries and compared with the population growth rate. Further the relation between trends, growth rate, area of urban extent and geographical location are assessed. Next, we calculated the changes in projected trends for different scenarios and quantified the uncertainty in climate models in determining the trends. Further changing magnitude and frequency of extreme temperature is assessed in terms of popularly used indices.

Temperature indices allow to understand effectively the changes in magnitude, duration and

frequency of extreme events (Sillmann et al., 2013). The Expert team of climate change detection and Indices (ETCCDI) developed a suit of indices to quantify the varying extremes in a region. These indices are widely used in literature, in both global and regional scales. Fourteen temperature indices that provide a comprehensive coverage of changes in magnitude, duration and frequency of extremes (LUO et al., 2020) were selected. The indices can be classified as: (a) absolute indices (TXx and TNn) (b) threshold indices (FD, ID) (c) percentile indices (TX90p and TN10p) and (d) duration indices (WSDI and CSDI). All the indices were calculated considering the base period as 1979-2008, for the four SSPs and for a given simulation and SSP, a linear line fit for each index and the slope is calculated. The changes in the index are noted on decadal basis. Uncertainty in the simulations has been assessed in modelling the future trend of extreme indices. The future period (2020-2100) is further divided into three time slices of 30 years each, that is, T1 (2021-2050), T2 (2041-2070) and T3 (2071-2100), to account for temporal variability.

Table 2.3: Categorisation and definitions of extreme temperature indices used in the analysis

Index Type	Index	Definition	Units
Absolute Indices	TXx	Annual maximum value of daily maximum temperature	°C
	TNn	Annual minimum value of daily minimum temperature	°C
Threshold Indices	ID	Annual number of days when TX < 0°C	Days
	FD	Annual number of days when TN < 0°C	Days
Duration Indices	WSDI	Annual number of days with at least six consecutive days where TX >90th Percentile	Days
	CSDI	Annual number of days with at least six consecutive days where TN >90th Percentile	Days
Percentile Indices	TX90p	Percentage of days in a year when TX > 90th percentile for a historical base period.	%
	TN10p	Percentage of days in a year when TN < 10th percentile for a historical base period.	%

2.3 Results

The average temperature of historical time series SCDNA and bias-corrected CMIP6 models is analyzed. The time-series shows a clear increasing trend for most of the cities (Figure 2.2). It is evident that relationships between urban features like elevation and area, can be noted. Cities in prairies have a milder slope compared to coastal and Great Lakes regions. It is noted that, cities with large population (Toronto, Montreal) have high slopes (of order 0.07°C per year). Most cities in Ontario, have high slope, with Ottawa having the highest slope (0.19°C per year). Though Ottawa and Edmonton have approximately same population, Edmonton has a mild slope (0.01°C per year). Further assessment of urban features and the historical annual mean trend, showed that there isn't a clear evidence of proportionality relationships between city area and population,

although elevation has an effect, with lower slopes for cities at higher elevations (Table A3). The bias-corrected future projections represented by the various shaded regions (Figure 2.2) also show a consistent increasing trend except for SSP1-2.6. Although, the scenario does exhibit an increasing trend in the first-half of the 21st century, the trend either plateaus or shows a slight decreasing trend towards the end of the century, as a result of the scenario's assumption of sustainable development and green future. Cities in the Canadian prairies have lower magnitude of annual mean temperatures, compared to other regions as they experienced colder winters historically.

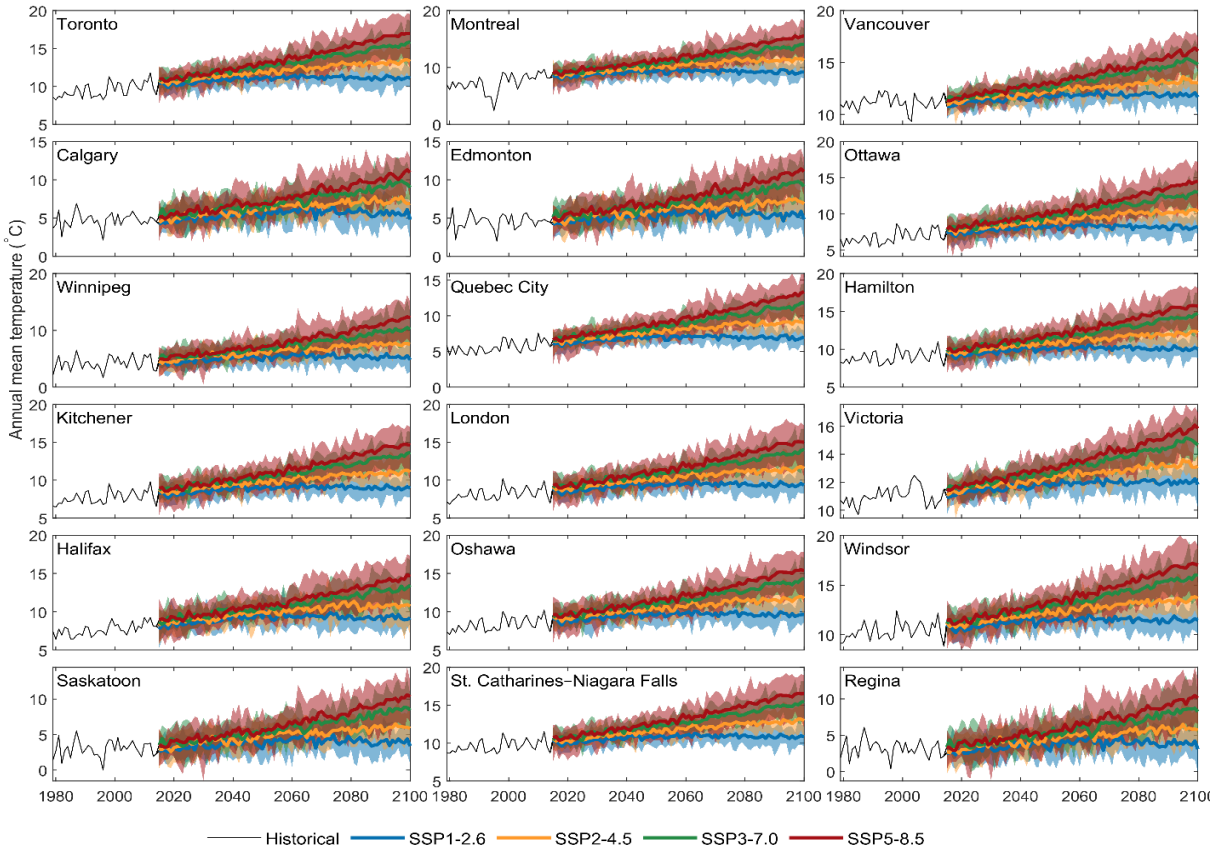

Figure 2.2: Annual average temperature for the historical (black line) and bias-corrected projected time-series for the four Shared Socio-economic Pathways (SSPs). The shaded region represents the 12 models in each emission scenario.

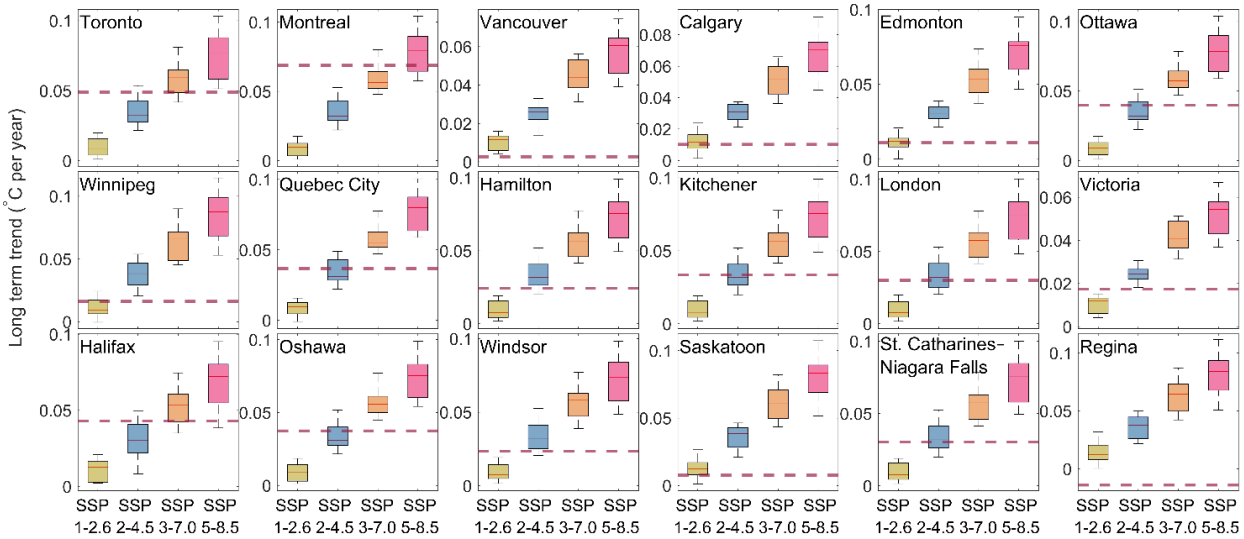

Figure 2.3: Long term trend in the annual mean temperature (°C per year) for different warming scenarios for the future. The red line shows the historical observed trend during 1979-2014.

Long term annual mean trends (Figure **2.3**), indicate that the slopes of the trend line are highest for SSP5-8.5 as it has the highest warming scenario. In the cities in prairies region, the historical trend line coincides or is below the trend projected by the SSP1-2.6 scenario. In the cities in the Great Lakes and North-eastern climate zones have a higher slope trend in the SSP2-4.5 scenario.

Substantial increase in average temperature by the end of 2100 is noted even for the least warming scenario, SSP1-2.6, for most of the cities (Figure A.1). An average increase of 0.7°C, 2.8°C, 5.3°C, and 6.7°C compared to the historical period is noted in SSP1-2.6, SSP2-4.5, SSP3-7.0 and SSP5-8.5 respectively in all the cities. Spatially, the increase for cities in the Canadian coastal areas, is smaller (from 2 to 4 °C) by the end of 2100. The cities in Quebec, belonging to the north-eastern climate zone, experience an increase very similar to the cities in the Great Lakes climate zone, an increase of 2.5 to 7.5 °C is noted. Though the average historical trends are milder in the prairies, the increase is much higher compared to the other regions.

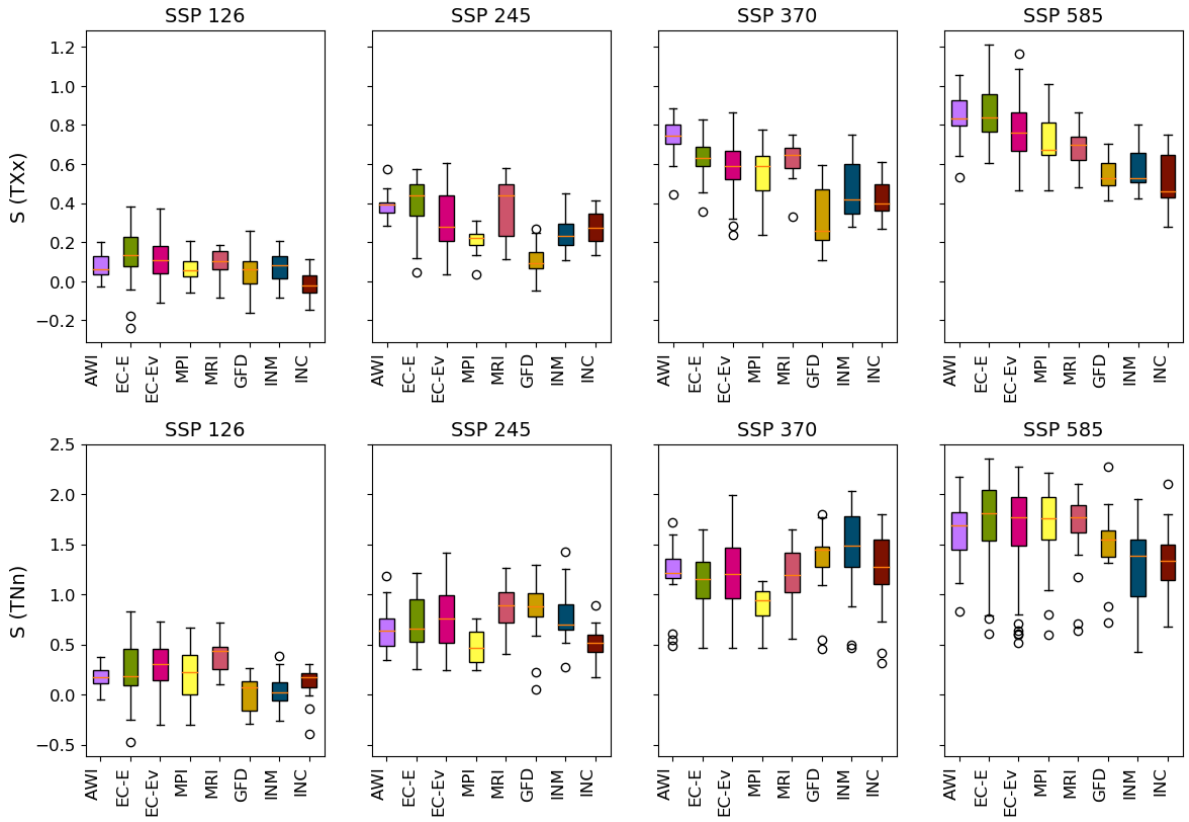

Figure 2.4: Slopes of TXx and TNn indices for individual models for all emission scenarios. The units of the rate of change are °C/decade.

The slopes of extreme temperature indices are plotted for all the individual models across all the cities, for every emission scenario (Figure 2.4, Figure A.5, Figure A.6, Figure A.7). The trends of TXx and TNn show that the AWI, MPI, and GFD are the models that have smaller variance across cities, whereas the other models, particularly EC-E and EC-Ev, exhibit a higher variance, as these two models have more than one variant label. Hence, rigorous model performance parameters should be used to quantitatively assess model performance.

The slopes of extreme temperature indices are also assessed for individual cities (Figure 2.5, Figure A.2, Figure A.3, Figure A. 4). Maximum temperature indices increase across emission scenarios, decreasing over the time-period T3 for SSP1-2.6 and increasing steadily across all the other emission scenarios, peaking at SSP5-8.5 in Figure 2.5. Increasing trends for WSDI and TX90p corelate with increasing TXx by showing an increase in percentage of hot days by 4.8 to 7.5% and duration of warm days by 20 to 30 days per decade as depicted in Figure 2.5. The minimum temperature indices like TN10p, CSDI and FD have decreasing trends of smaller magnitudes.

Increasing trends are observed for TXx and TNn, with the trend for TNn being higher at 2 °C, compared to a maximum increase of 1.5 °C for TXx.

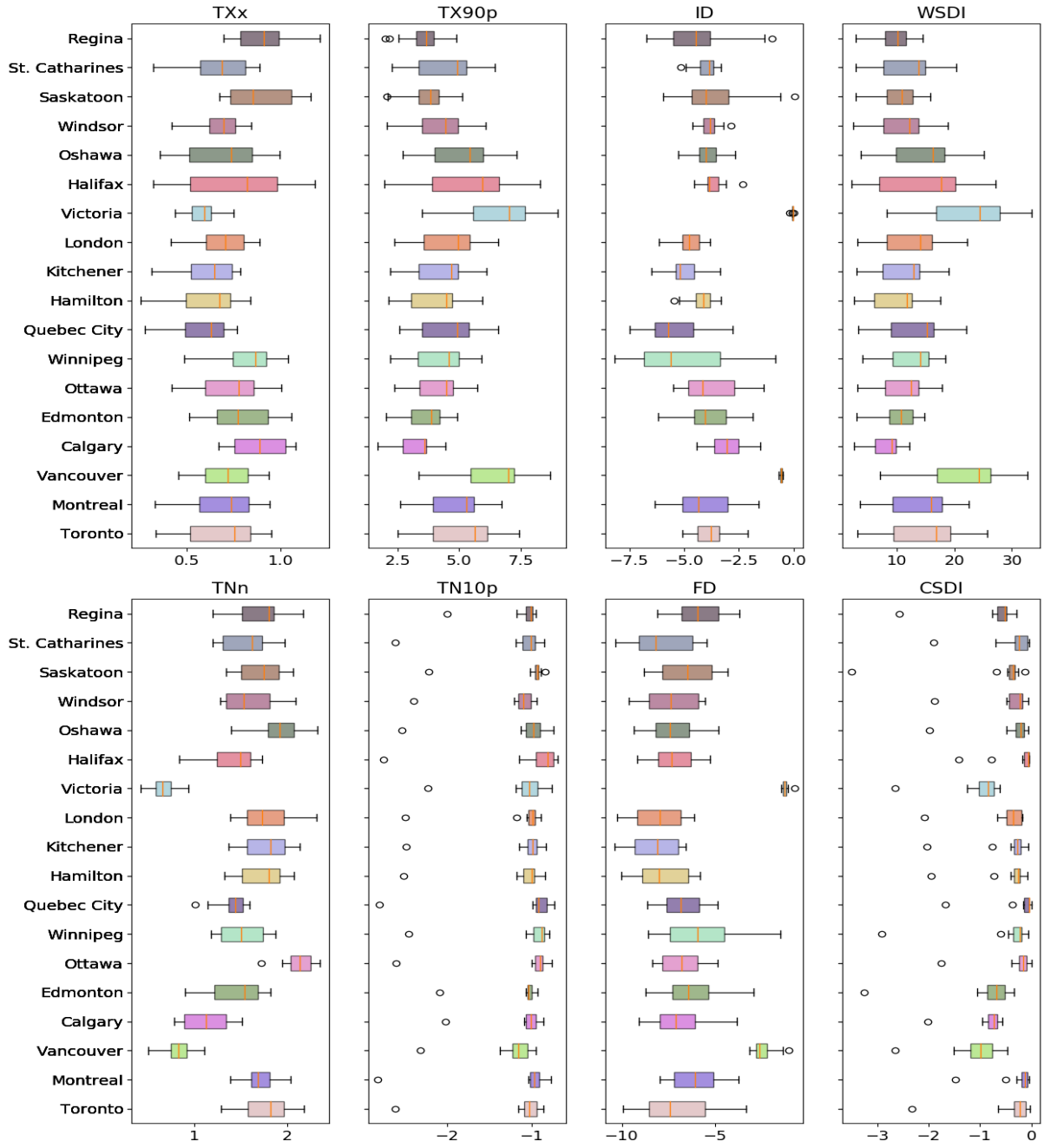

Figure 2.5: Indices Slopes for CMIP6 models as shown for the emission scenario SSP5-8.5. The units of the indices are °C/decade for TXx and TNn, days/decade for WSDI, CSDI, ID and FD and %/decade for TX90p and TN10p.

Spatial variation of indices offers substantial insight into future temperature patterns across

Canadian cities. The indices trend for each city is represented by the mean trend of all the models for this city. A slight increasing (or decreasing) trend approximately 0.1°C is noted for the absolute indices for SSP1-2.6 (Figure A.8). The max-indices steadily increase with increasing emission scenarios. It is also noted that the cities in the Canadian prairies, experience the highest increase in absolute indices' trends over both SSP2-4.5 and SSP3-7.0 (Figure A.9, Figure A.10), whereas the cities in the Great Lakes, show the highest increase in SSP1-2.6 scenario. The other maximum temperature indices (TX90p and WSDI), show that the Canadian coastal cities have the highest trends in all the emission scenarios. The minimum temperature indices show slim decreasing trends, with the trend intensifying marginally with increasing emission scenario (Figure A.9, Figure A.10)

The Spatial patterns for emission scenario of SSP5-8.5 (Figure 2.6), are similar to the trends in the emission scenarios like SSP3-7.0 and even SSP2-4.5. The absolute indices peak in the cities in Canadian prairies climate zone, but other maximum temperature indices (TX90p, WSDI) exhibit higher increasing rates for cities in the Canadian coasts.

The trends of ID and FD show a decrease over most of the cities, except Vancouver and Victoria, however the trend of CSDI shows only a marginal decreasing trend of -1 to -1.2 days per decade. The highest decrease of ID is observed in Saskatoon, and surrounding cities in the prairies. The cities in the east-coast like Halifax, in the North-eastern climate zone like Quebec City and surrounding cities in the Great Lakes zone, also experience a decrease of 3.5 to 4.2 days per decade.

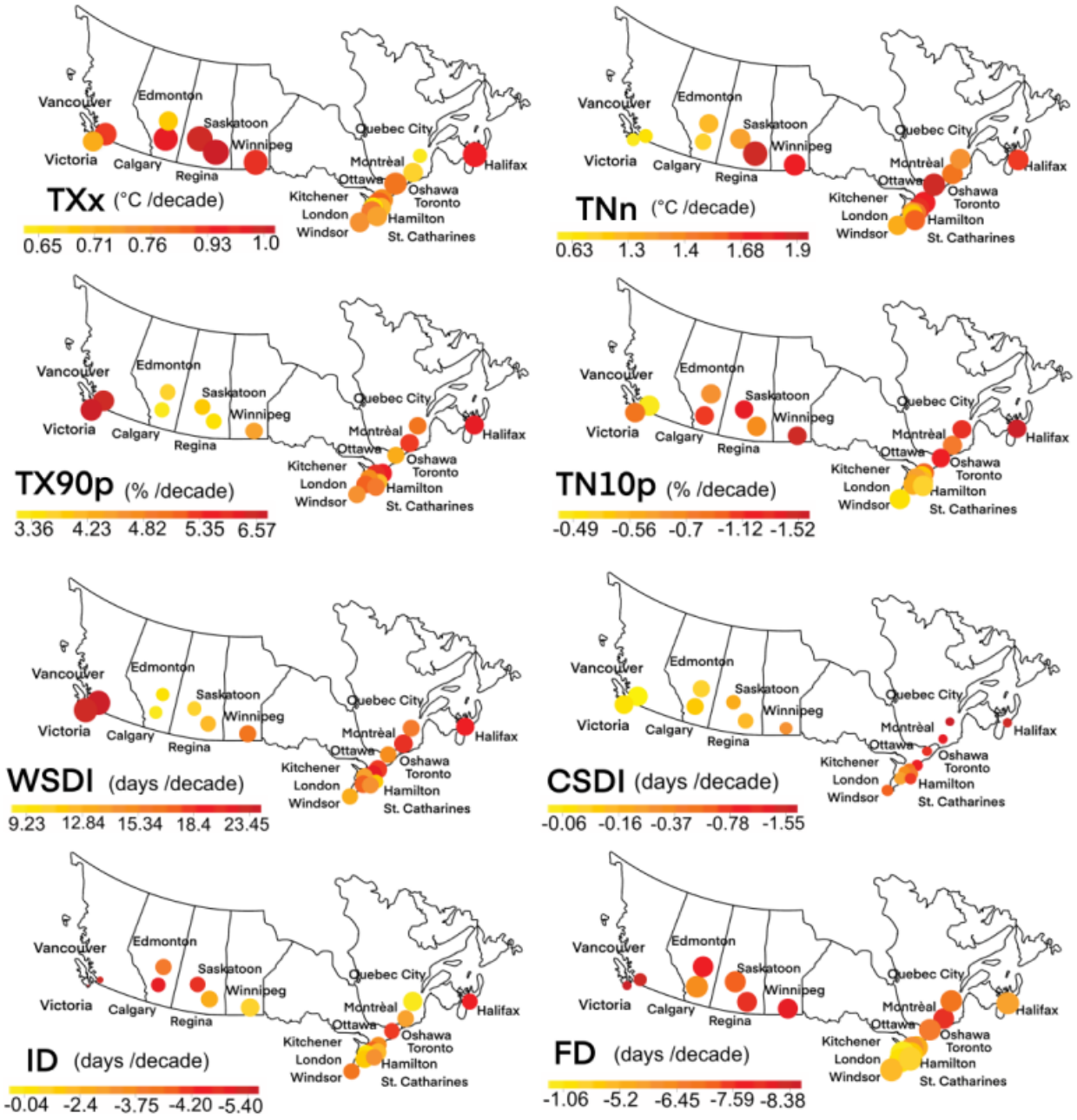

Figure 2.6: Spatial trends variation of all 8 indices for the emission scenario SSP5-8.5. The size of the dots is proportional to the magnitude of the trend.

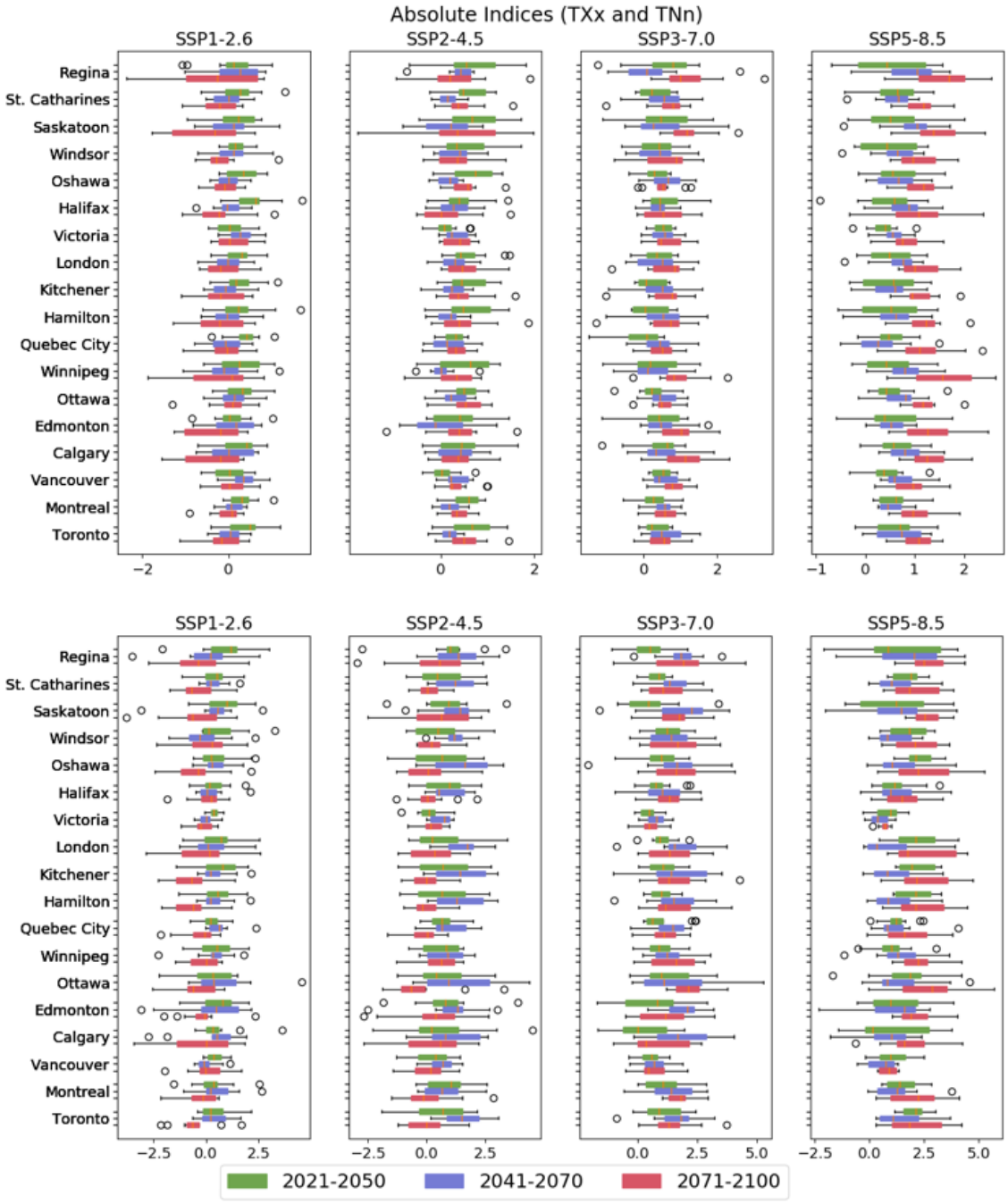

Figure 2.7: Boxplots for Absolute indices TXx (above) and TNn (below), the units of TX and TN are °C /decade.

The trends of TXx and TNn are inconsistent throughout the time-period of study and are presented in three separate time periods of 2021-2050 (T1), 2041-2070 (T2) and 2071-2100 (T3). The boxplots shown in Figure 2.7 of Absolute indices (TXx and TNn), show an increasing trend for both the SSP scenarios of 2-4.5, 3-7.0, and 5-8.5, which are used extensively for decision making

for mitigation measures in urban areas (Daniel et al., 2019) whereas the scenario of SSP-1-2.6 showing a decreasing trend. The increase of TXx between the time periods of T1to T3, is a median of 0.5 to 0.6 °C in the T2 time-period to almost 1.10 °C per decade in the T3 period in the scenario of SSP5-8.5, and this trend is even higher for TNn, translating to an increase in minimum temperature of over 1.90 °C per decade in T3 in the frigid regions of Canadian prairies. The relative change of magnitudes is greater for the cities of the Canadian prairies like Regina, Saskatoon and Winnipeg, and Calgary and Edmonton, situated at the region's periphery. The cities in the climate zones of the Great Lakes, also experience a maximum temperature increase (TXx) of about 1°C per decade, and a minimum temperature increase of even 2 °C of the TNn index, in the SSP5-8.5 scenario for time-period T3.

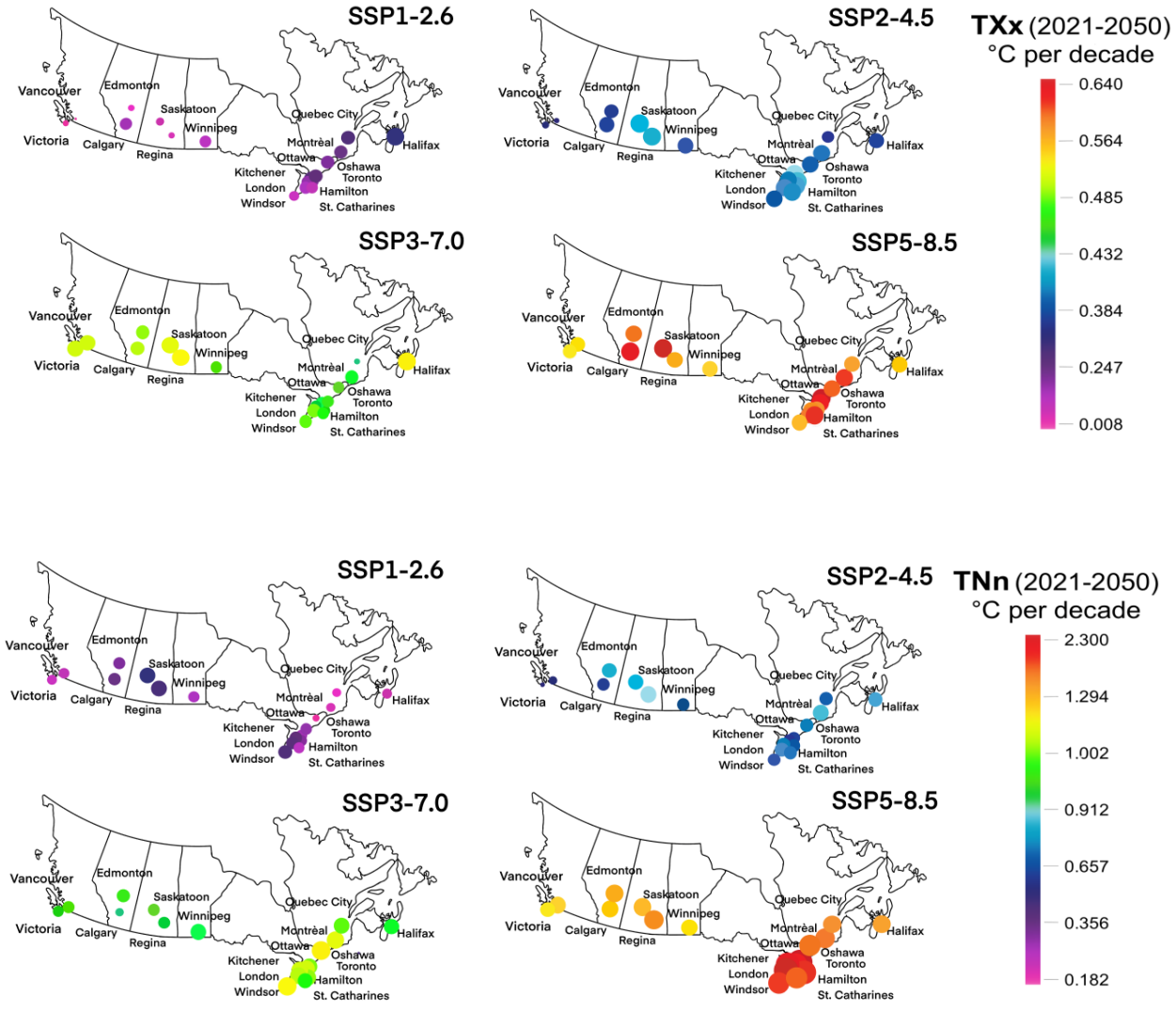

Figure 2.8: Spatial Variation of TXx and TNn indices for the decades T1

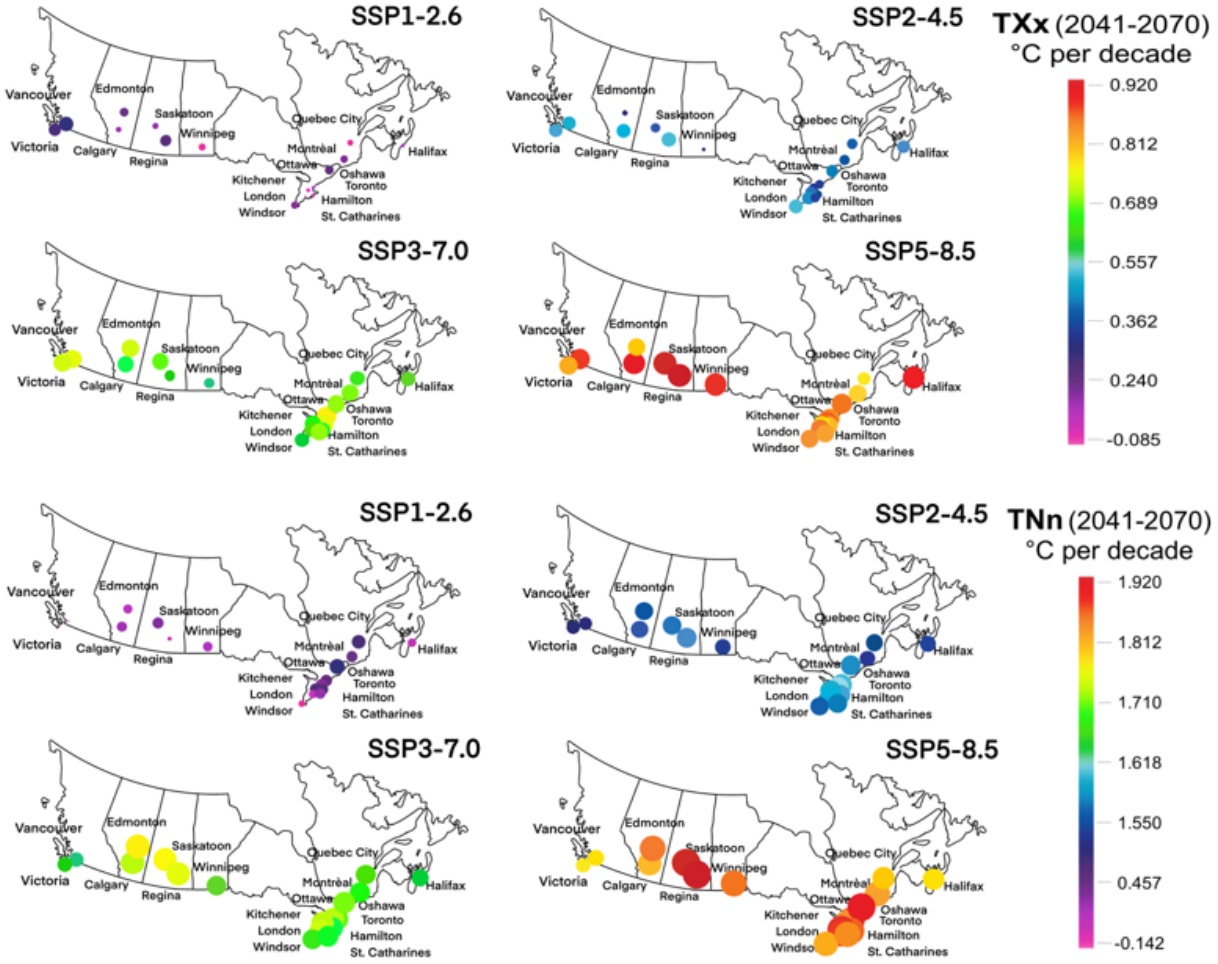

Figure 2.9: Spatial Variation of TXx and TNn indices for time-period T2

The mean absolute magnitude of all the CMIP6 models for one scenario of an index value is shown as the spatial variation of for the indices TXx and TNn through (Figure 2.8, Figure 2.9 and Figure **2.10**). The TXx and TNn indices have a mean increase by 0.91 and 1.52 °C per decade across the time-period of study. The spatial variation varies a great deal throughout the twenty-first century. Figure 2.8 shows that the average increase in both the TXx and TNn indices are 0.45 and 0.91 °C increase per decade in the highest emission scenario. The lowest emission scenario, SSP1-2.6 in fact, shows a decreasing trend through, to the decades of T3, as demonstrated by Figure 2.10. In the decades of T2, the increase of TXx and TNn is as high as 0.92 and 1.920, higher than the average for the time-period of 2015-2100. The cities that experience the highest increase in the decades of T2 are the Saskatoon, Regina, and Winnipeg, situated in the Canadian prairies. The

cities in the Great Lakes region in Ontario also, experience an increase of 0.85 °C and 1.86 °C per decade in the TXx and TNn indices respectively. In the time-period T3, the increase per decade of TXx and TNn is as high as 1.53 °C and 2.5 °C in the SSP5-8.5 scenario. Both the higher emission scenarios, SSP3-7.0 and SSP5-8.5, have the high increasing trend in the latter part of the twenty-first century.

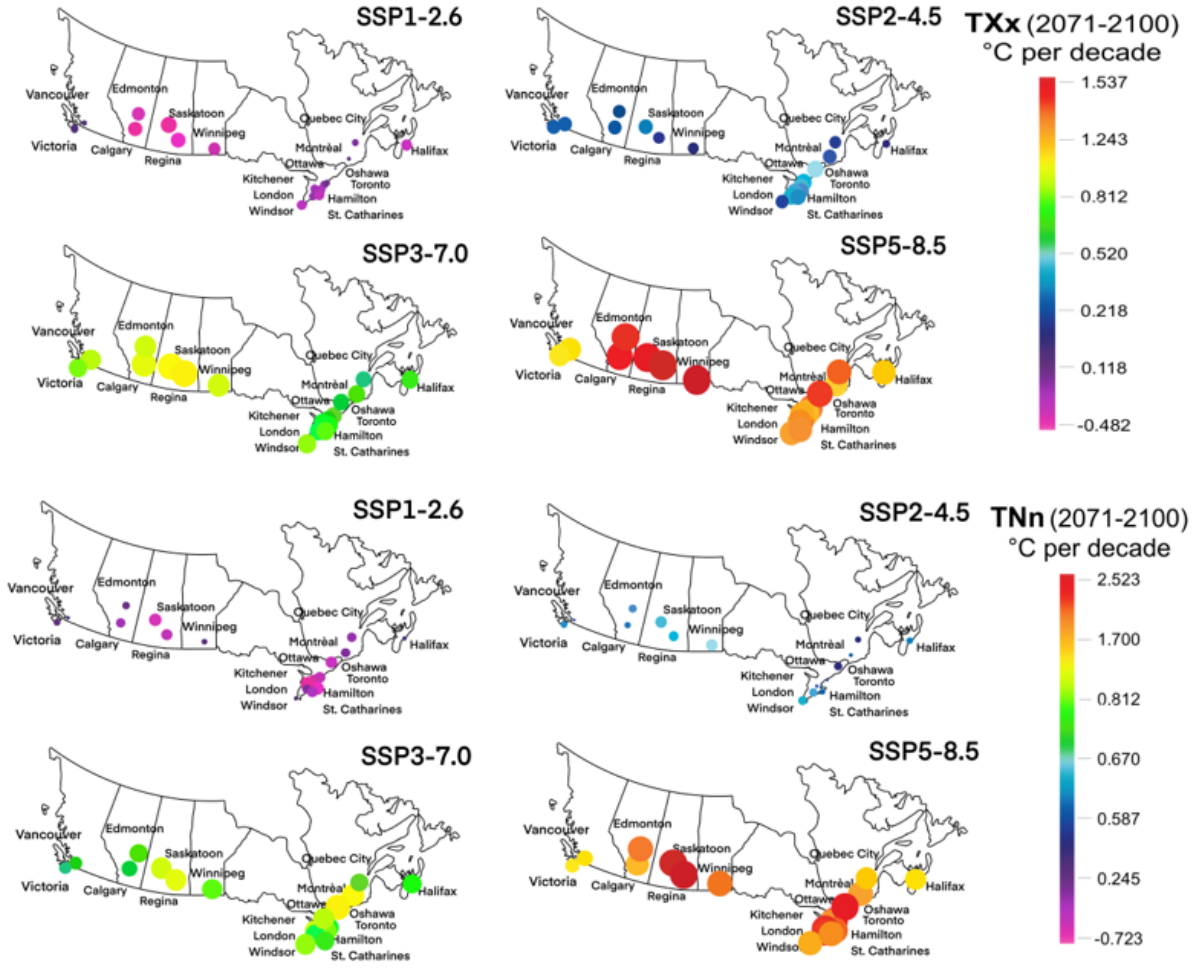

Figure 2.10: Spatial Variation of TXx and TNn indices for time-period T3

Percentile index TX90p experiences an increasing trend throughout the future period of 2015-2100. TX90p index has a median increase of 4.5 % per decade for majority of the cities (Figure 2.5) with west coast cities like Vancouver and Victoria, experiencing a higher increase of about 5 % increase per decade. The spatial trends show a consistent increasing trend for all the emission scenarios, with the highest increase of 6.23% per decade for the Pacific coastal cities of Victoria

and Vancouver, and the Atlantic coastal city of Halifax. Cities in the Canadian prairies also experience a 5% increase per decade, in the highest scenario of SSP5-8.5 (Figure 2.6)

The TN10p index shows a decreasing trend across all emission scenarios (Figure A.2, Figure A.3, Figure A. 4). Unlike TX90p, the variation of the trend is not high. Across the time-period of study (2015-2100) the decreasing trend varies between 0.2 and 1.5% decrease per decade. No substantial difference is noticed in the variation of spatial pattern for the TN10p index, as most cities across the both sides of the Canadian coast, the prairies and the Great Lakes region experiencing a decreasing trend of 1.2% per decade over the emission scenarios of SSP3-7.0 and SSP5-8.5.

Threshold indices like Icing days (ID) and Frost days (FD) indicate the trend of number of days below a threshold of maximum and minimum temperature projections. Both the indices exhibit a decreasing of the indices, all the scenarios through the 2015-2100 time-period indicating warmer maximum and minimum temperatures in all climate zones. The indices show that cities in the Canadian prairies like Saskatoon, Regina and Winnipeg have a median change of -4.5 to -7.5 days/decade in SSP3-7.5 and SSP58.5 in the ID index. The index FD also has a decreasing trend of -8.5 days in the SSP5-8.5 scenario, a correlation with increasing TNn index in the cities in the Canadian prairies (Figure 2.4).

Changes in the CSDI index is steady decrease of cold spell durations throughout the cities of interest. The emission scenarios SSP3-7.0 and SSP5-8.5 for all the cities experience a duration change of 0.5-1 day/decade (Figure A.2, Figure A.3, Figure A. **4** and Figure 2.6). The spatial variation of the CSDI index is uniform throughout, like the WSDI index, the CSDI index has a direct correlation with the TN10p index, although its reduction rates are lower than the increasing rate of WSDI.

2.4 Discussion

All the results clearly indicate that as the magnitude of extreme temperature indices varies across emission scenarios (Seneviratne et al., 2016). The warming trends intensify with increasing emission scenario i.e., from SSP-1-26 to SSP-5-8.5. Long-term future annual mean trends indicate a significant increase, from historical trends. The trends in most cities are captured by the SSP1-2.6 (cities in the prairies or coastal regions) or the SSP2-4.5 (cities in the Great Lakes and the northeastern climate regions) scenario, indicating that the higher emission scenarios (SSP3-70 and

SSP5-85) predict higher warming trends. The historical trend in Ottawa is however, not captured well by any emission scenario.

Projected long-term trends across Canadian cities are being supplemented by previous studies that indicate the average mean-temperature over Canada is expected to rise by 2°C in the lowest emission scenario, by the mid-2050s and more than 6°C in the higher emission scenario, by the end of the twenty-first century, with Southern Canadian provinces experiencing an increase of 7-8 C based on the reference base period of 1985-2005. Intuitively, the increase of maximum temperature will be even higher (Bush,E & Flato,G, 2019) as the highest increasing trend of 0.91°C and 1.2°C per decade, for TXx and TNn across all cities for the highest emission scenario (Figure 2.6) which depict the spatial patterns for the future time-period of reference.

Both the Absolute indices (TXx and TNn) show an increasing trend, where the magnitude of increase of TNn, is higher than TXx for all the cities involved in the study, in accordance to previous research on the global trends of TNn (Sillmann et al., 2013). The spatial patterns of annual maximum temperature (TXx) presented in Figure A.8, Figure A.9 and Figure A.10 show that the cities in the Prairies climate zone have a higher warming trend in the scenario SSP-3-7.0, and that trend slows down in the scenario SSP-5-8.5, where the cities in the great lake climate zone have the highest magnitude of warming in the 2070-2100 decades. This is consistent with the findings in literature; the warming trend over the Canadian prairies shows an increase in mean temperature of upto of 7.2 °C in the 2060s and the 2070s in the RCP8.5 scenario (which is similar SSP5-8.5 scenario) (Zhou et al., 2018). The results in TX90p are consistent with the WSDI results, the cities experience the highest percentage increase for both the indices across the scenarios SSP3-7.0 and SSP5-8.5. TN10p shows a decreasing trend, a decrease of 1 % per decade, is consistent with an increase in minimum temperature. The trends in percentile indices, indicate an increase in magnitude of higher temperature extremes i.e., increase in temperatures greater than 90^{th} percentile value of base period, but only a marginal decrease in temperature extremes i.e., temperatures below 10^{th} percentile value of base period. The significance of the results of percentile indices is that although there is an increase in maximum temperature extreme events in Canada, the frequency of lower temperature extremes (in winter) will continue to persist throughout twenty-first century, just like the observed increasing trend of minimum temperature warming over Southern Canada (Bonsal et al., 2001; Peacock, 2012). The coastal cities of Victoria and Vancouver do not see any change in either of the threshold indices (ID or FD), as their maximum and minimum temperatures

do not fall below the threshold value of 0°C.

2.5 Summary and Conclusion

Bias-corrected TX and TN CMIP6 datasets across emission scenarios except the most optimistic scenario in SSP1-2.6, predict an irregular warming of large Canadian population centers, consistent with previous studies on CMIP projections in Canada. The annual mean (Figure 2.2) increases with increasing emission scenario, and so are the warming trends of various temperature indices analyzed in the paper. All the CMIP6 models agree with the trends projected by extreme temperature indices, for e.g., all the models simultaneously predict an increasing trend of TXx index or a decreasing trend of TN10p index. The rate of increase of TNn is higher than TXx across emission scenarios and cities, and its spatial variation points towards a higher rate of warming minimum temperatures in the cities in the Canadian prairies and the Great Lakes climate zones.

Indices computed from TX (TXx, TX90p, WSDI and ID), have an increasing trend across emission scenarios, except the SSP1-2.6 scenario. The Indices although predict an initial increasing trend for the SSP1-2.6 scenario, over the decades in T1, project a decreasing trend thereafter. Spatial patterns of TX indices (mean trend of all the models) show that the largest increase in magnitude of the TXx index is in the cities in the prairie climate zone Saskatoon, Regina, Winnipeg, Calgary and Edmonton. Although the magnitude of increasing trend in TXx or the TNn is not very high, over the coastal cities of Victoria, Vancouver and Halifax, higher frequency of warmer temperatures is corroborated by the trends of the TX90p and the WSDI indices. Increasing rates of the ID and the FD, consistently show that the both the cities in the Canadian prairies and the Great Lakes climate zones, have higher warming trends across higher emission scenarios (SSP3-7.0 and SSP5-85), and amongst other Canadian cities involved in the study. Finally, the indices of TN10p and CSDI, do not correlate with the increasing rate TNn. Although both TN10p and CSDI have marginal decreasing trends across all the cities in Canada.

References

Alexander, L. V., Zhang, X., Peterson, T. C., Caesar, J., Gleason, B., Tank, A. M. G. K., et al. (2006). Global observed changes in daily climate extremes of temperature and precipitation. *Journal of Geophysical Research: Atmospheres*, *111*(D5). https://doi.org/10.1029/2005JD006290

Allen, S. M. J., Gough, W. A., & Mohsin, T. (2015). Changes in the frequency of extreme temperature records for Toronto, Ontario, Canada. *Theoretical and Applied Climatology*, *119*(3), 481–491. https://doi.org/10.1007/s00704-014-1131-1

Anandhi, A., Frei, A., Pierson, D. C., Schneiderman, E. M., Zion, M. S., Lounsbury, D., & Matonse, A. H. (2011). Examination of change factor methodologies for climate change impact assessment. *Water Resources Research*, *47*(3). https://doi.org/10.1029/2010WR009104

Ashour, S. K., & Abdel-hameed, M. A. (2010). Approximate skew normal distribution. *Journal of Advanced Research*, *1*(4), 341–350. https://doi.org/10.1016/j.jare.2010.06.004

Azzalini, A. (2011). Skew-Normal Distribution. In M. Lovric (Ed.), *International Encyclopedia of Statistical Science* (pp. 1342–1344). Berlin, Heidelberg: Springer. https://doi.org/10.1007/978-3-642-04898-2_523

Barrow, E. M., & Sauchyn, D. J. (2017). An analysis of the performance of RCMs in simulating current climate over western Canada. *International Journal of Climatology*, *37*(S1), 640–658. https://doi.org/10.1002/joc.5028

Bastidas-Arteaga, E., Chateauneuf, A., Sánchez-Silva, M., Bressolette, Ph., & Schoefs, F. (2010). Influence of weather and global warming in chloride ingress into concrete: A stochastic

approach. *Structural Safety*, *32*(4), 238–249. https://doi.org/10.1016/j.strusafe.2010.03.002

Belda Revert, A., De Weerdt, K., Hornbostel, K., & Geiker, M. R. (2018). Carbonation-induced corrosion: Investigation of the corrosion onset. *Construction and Building Materials*, *162*, 847–856. https://doi.org/10.1016/j.conbuildmat.2017.12.066

Bonsal, B. R., Zhang, X., Vincent, L. A., & Hogg, W. D. (2001). Characteristics of Daily and Extreme Temperatures over Canada. *Journal of Climate*, *14*(9), 1959–1976. https://doi.org/10.1175/1520-0442(2001)014<1959:CODAET>2.0.CO;2

Buishand, T. A., & Brandsma, T. (1999). Dependence of precipitation on temperature at Florence and Livorno (Italy). *Climate Research*, *12*(1), 53–63. Retrieved from http://www.jstor.org/stable/24865998

Bush,E & Flato,G. (2019). *Canada's Changing Climate Report*. Natural Resources Canada. Retrieved from https://www.nrcan.gc.ca/climate-change/impacts-adaptations/canadas-changing-climate-report/21177

Cannon, A. J., Sobie, S. R., & Murdock, T. Q. (2015). Bias Correction of GCM Precipitation by Quantile Mapping: How Well Do Methods Preserve Changes in Quantiles and Extremes? *Journal of Climate*, *28*(17), 6938–6959. https://doi.org/10.1175/JCLI-D-14-00754.1

Chen, J., Brissette, F. P., Chaumont, D., & Braun, M. (2013). Finding appropriate bias correction methods in downscaling precipitation for hydrologic impact studies over North America. *Water Resources Research*, *49*(7), 4187–4205. https://doi.org/10.1002/wrcr.20331

Choi, Y.-Y., Suh, M.-S., & Park, K.-H. (2014). Assessment of Surface Urban Heat Islands over Three Megacities in East Asia Using Land Surface Temperature Data Retrieved from

COMS. *Remote Sensing*, *6*(6), 5852–5867. https://doi.org/10.3390/rs6065852

Daniel, M., Lemonsu, A., Déqué, M., Somot, S., Alias, A., & Masson, V. (2019). Benefits of explicit urban parameterization in regional climate modeling to study climate and city interactions. *Climate Dynamics*, *52*(5), 2745–2764. https://doi.org/10.1007/s00382-018-4289-x

Dave Sauchyn & Debra Davidson. (2020). *Canada in a Changing Climate: Regional Perspectives Report* (p. 72).

Diffenbaugh, N. S., & Giorgi, F. (2012). Climate change hotspots in the CMIP5 global climate model ensemble. *Climatic Change*, *114*(3), 813–822. https://doi.org/10.1007/s10584-012-0570-x

Ehret, U., Zehe, E., Wulfmeyer, V., Warrach-Sagi, K., & Liebert, J. (2012). HESS Opinions "Should we apply bias correction to global and regional climate model data?" *Hydrology and Earth System Sciences*, *16*(9), 3391–3404. https://doi.org/10.5194/hess-16-3391-2012

Eyring, V., Bony, S., Meehl, G. A., Senior, C. A., Stevens, B., Stouffer, R. J., & Taylor, K. E. (2016). Overview of the Coupled Model Intercomparison Project Phase 6 (CMIP6) experimental design and organization. *Geoscientific Model Development*, *9*(5), 1937–1958. https://doi.org/10.5194/gmd-9-1937-2016

Fortune, M. K., Mustard, C. A., Etches, J. J. C., & Chambers, A. G. (2013). Work-attributed Illness Arising From Excess Heat Exposure in Ontario, 2004–2010. *Canadian Journal of Public Health*, *104*(5), e420–e426. https://doi.org/10.17269/cjph.104.3984

Gallo, K., & Xian, G. (2014). Application of spatially gridded temperature and land cover data sets for urban heat island analysis. *Urban Climate*, *8*, 1–10.

https://doi.org/10.1016/j.uclim.2014.04.005

Gaur, A., Eichenbaum, M. K., & Simonovic, S. P. (2018). Analysis and modelling of surface Urban Heat Island in 20 Canadian cities under climate and land-cover change. *Journal of Environmental Management*, *206*, 145–157. https://doi.org/10.1016/j.jenvman.2017.10.002

Gosling, S. N., Lowe, J. A., McGregor, G. R., Pelling, M., & Malamud, B. D. (2009). Associations between elevated atmospheric temperature and human mortality: a critical review of the literature. *Climatic Change*, *92*(3), 299–341. https://doi.org/10.1007/s10584-008-9441-x

Government of Canada, S. C. (2015, April 13). Canada goes urban. Retrieved April 13, 2020, from https://www150.statcan.gc.ca/n1/pub/11-630-x/11-630-x2015004-eng.htm

Graham, L. P., Andréasson, J., & Carlsson, B. (2007). Assessing climate change impacts on hydrology from an ensemble of regional climate models, model scales and linking methods – a case study on the Lule River basin. *Climatic Change*, *81*(1), 293–307. https://doi.org/10.1007/s10584-006-9215-2

Grillakis, M. G., Koutroulis, A. G., & Tsanis, I. K. (2011). Climate change impact on the hydrology of Spencer Creek watershed in Southern Ontario, Canada. *Journal of Hydrology*, *409*(1), 1–19. https://doi.org/10.1016/j.jhydrol.2011.06.018

Grillakis, M. G., Koutroulis, A. G., Daliakopoulos, I. N., Tsanis, I. K., & Tsanis, I. K. (2017). A method to preserve trends in quantile mapping bias correction of climate modeled temperature. *Earth System Dynamics*, *8*, 889–900. https://doi.org/10.5194/esd-8-889-2017

Guo, L.-Y., Gao, Q., Jiang, Z.-H., & Li, L. (2018). Bias correction and projection of surface air temperature in LMDZ multiple simulation over central and eastern China. *Advances in*

Climate Change Research, *9*(1), 81–92. https://doi.org/10.1016/j.accre.2018.02.003

Haerter, J. O., Hagemann, S., Moseley, C., & Piani, C. (2011). Climate model bias correction and the role of timescales. *Hydrology and Earth System Sciences*, *15*(3), 1065–1079. https://doi.org/10.5194/hess-15-1065-2011

Ines, A. V. M., & Hansen, J. W. (2006). Bias correction of daily GCM rainfall for crop simulation studies. *Agricultural and Forest Meteorology*, *138*(1), 44–53. https://doi.org/10.1016/j.agrformet.2006.03.009

Jury, M. W., Prein, A. F., Truhetz, H., & Gobiet, A. (2015). Evaluation of CMIP5 Models in the Context of Dynamical Downscaling over Europe. *Journal of Climate*, *28*(14), 5575–5582. https://doi.org/10.1175/JCLI-D-14-00430.1

Katz, R. W., & Brown, B. G. (1992). Extreme events in a changing climate: Variability is more important than averages. *Climatic Change*, *21*(3), 289–302. https://doi.org/10.1007/BF00139728

Keatinge, W. R., & Donaldson, G. C. (2004, November). The impact of global warming on health and mortality. *Southern Medical Journal*, *97*(11), 1093+. Retrieved from http://link.gale.com/apps/doc/A126076453/EAIM?sid=bookmark-EAIM&xid=2396cc48

Knutti, R., & Sedláček, J. (2013). Robustness and uncertainties in the new CMIP5 climate model projections. *Nature Climate Change*, *3*(4), 369–373. https://doi.org/10.1038/nclimate1716

Kolb, S., Radon, K., Valois, M.-F., Héguy, L., & Goldberg, M. S. (2007). The Short-Term Influence of Weather on Daily Mortality in Congestive Heart Failure. *Archives of Environmental & Occupational Health*, *62*(4), 169–176. https://doi.org/10.3200/AEOH.62.4.169-176

Lauwaet, D., Hooyberghs, H., Maiheu, B., Lefebvre, W., Driesen, G., Looy, S. V., & Ridder, K. D. (2015). Detailed Urban Heat Island Projections for Cities Worldwide: Dynamical Downscaling CMIP5 Global Climate Models. *Climate*, *3*(2), 391–415. https://doi.org/10.3390/cli3020391

Li, H., Sheffield, J., & Wood, E. F. (2010). Bias correction of monthly precipitation and temperature fields from Intergovernmental Panel on Climate Change AR4 models using equidistant quantile matching. *Journal of Geophysical Research: Atmospheres*, *115*(D10). https://doi.org/10.1029/2009JD012882

Li, Z., Huang, G., Huang, W., Lin, Q., Liao, R., & Fan, Y. (2018). Future changes of temperature and heat waves in Ontario, Canada. *Theoretical and Applied Climatology*, *132*(3), 1029–1038. https://doi.org/10.1007/s00704-017-2123-8

LUO, N., GUO, Y., GAO, Z., CHEN, K., & CHOU, J. (2020). Assessment of CMIP6 and CMIP5 model performance for extreme temperature in China. *Atmospheric and Oceanic Science Letters*, *13*(6), 589–597. https://doi.org/10.1080/16742834.2020.1808430

Martin, S. L., Cakmak, S., Hebbern, C. A., Avramescu, M.-L., & Tremblay, N. (2012). Climate change and future temperature-related mortality in 15 Canadian cities. *International Journal of Biometeorology*, *56*(4), 605–619. https://doi.org/10.1007/s00484-011-0449-y

Maurer, E. P., Brekke, L., Pruitt, T., & Duffy, P. B. (2007). Fine-resolution climate projections enhance regional climate change impact studies. *Eos, Transactions American Geophysical Union*, *88*(47), 504–504. https://doi.org/10.1029/2007EO470006

McMichael, A. J., Woodruff, R. E., & Hales, S. (2006). Climate change and human health: present and future risks. *The Lancet*, *367*(9513), 859–869. https://doi.org/10.1016/S0140-

6736(06)68079-3

Meehl, G. A., & Tebaldi, C. (2004). More Intense, More Frequent, and Longer Lasting Heat Waves in the 21st Century. *Science*, *305*(5686), 994–997. Retrieved from https://www.jstor.org/stable/3837565

Murray, V., & Ebi, K. L. (2012). IPCC Special Report on Managing the Risks of Extreme Events and Disasters to Advance Climate Change Adaptation (SREX). *Journal of Epidemiology and Community Health (1979-)*, *66*(9), 759–760. Retrieved from http://www.jstor.org/stable/23269103

Notaro, M., Bennington, V., & Lofgren, B. (2015). Dynamical Downscaling-Based Projections of Great Lakes Water Levels*+. *Journal of Climate*, *28*(24), 9721–9745. https://doi.org/10.1175/JCLI-D-14-00847.1

Papalexiou, S. M., AghaKouchak, A., Trenberth, K. E., & Foufoula-Georgiou, E. (2018). Global, Regional, and Megacity Trends in the Highest Temperature of the Year: Diagnostics and Evidence for Accelerating Trends. *Earth's Future*, *6*(1), 71–79. https://doi.org/10.1002/2017EF000709

Peacock, S. (2012). Projected Twenty-First-Century Changes in Temperature, Precipitation, and Snow Cover over North America in CCSM4. *Journal of Climate*, *25*(13), 4405–4429. https://doi.org/10.1175/JCLI-D-11-00214.1

Pengelly, L. D., Campbell, M. E., Cheng, C. S., Fu, C., Gingrich, S. E., & Macfarlane, R. (2007). Anatomy of Heat Waves and Mortality in Toronto. *Canadian Journal of Public Health*, *98*(5), 364–368. https://doi.org/10.1007/BF03405420

Perkins, S. E., & Alexander, L. V. (2013). On the Measurement of Heat Waves. *Journal of Climate*,

26(13), 4500–4517. https://doi.org/10.1175/JCLI-D-12-00383.1

Piani, C., Weedon, G. P., Best, M., Gomes, S. M., Viterbo, P., Hagemann, S., & Haerter, J. O. (2010). Statistical bias correction of global simulated daily precipitation and temperature for the application of hydrological models. *Journal of Hydrology*, *395*(3), 199–215. https://doi.org/10.1016/j.jhydrol.2010.10.024

Piao, S., Ciais, P., Huang, Y., Shen, Z., Peng, S., Li, J., et al. (2010). The impacts of climate change on water resources and agriculture in China. *Nature*, *467*(7311), 43–51. https://doi.org/10.1038/nature09364

Plummer, D. A., Caya, D., Frigon, A., Côté, H., Giguère, M., Paquin, D., et al. (2006). Climate and Climate Change over North America as Simulated by the Canadian RCM. *Journal of Climate*, *19*(13), 3112–3132. https://doi.org/10.1175/JCLI3769.1

Power, S., Delage, F., Wang, G., Smith, I., & Kociuba, G. (2017). Apparent limitations in the ability of CMIP5 climate models to simulate recent multi-decadal change in surface temperature: implications for global temperature projections. *Climate Dynamics*, *49*(1), 53–69. https://doi.org/10.1007/s00382-016-3326-x

Reichstein, M., Bahn, M., Ciais, P., Frank, D., Mahecha, M. D., Seneviratne, S. I., et al. (2013). Climate extremes and the carbon cycle. *Nature*, *500*(7462), 287–295. https://doi.org/10.1038/nature12350

Rizwan, A. M., Dennis, L. Y. C., & Liu, C. (2008). A review on the generation, determination and mitigation of Urban Heat Island. *Journal of Environmental Sciences*, *20*(1), 120–128. https://doi.org/10.1016/S1001-0742(08)60019-4

Rummukainen, M. (2010). State-of-the-art with regional climate models. *WIREs Climate Change*,

1(1), 82–96. https://doi.org/10.1002/wcc.8

Schar, C., Vidale, P. L., Luthi, D., Frei, C., Haberli, C., Liniger, M. A., & Appenzeller, C. (2004). The role of increasing temperature variability in European summer heatwaves. *Nature*, *427*(6972), 332-. Retrieved from http://link.gale.com/apps/doc/A186371710/EAIM?u=usaskmain&sid=zotero&xid=e5e58c2c

Seneviratne, S. I., Donat, M. G., Pitman, A. J., Knutti, R., & Wilby, R. L. (2016). Allowable CO 2 emissions based on regional and impact-related climate targets. *Nature*, *529*(7587), 477–483. https://doi.org/10.1038/nature16542

Sillmann, J., Kharin, V. V., Zhang, X., Zwiers, F. W., & Bronaugh, D. (2013). Climate extremes indices in the CMIP5 multimodel ensemble: Part 1. Model evaluation in the present climate. *Journal of Geophysical Research: Atmospheres*, *118*(4), 1716–1733. https://doi.org/10.1002/jgrd.50203

Sillmann, J., Kharin, V. V., Zwiers, F. W., Zhang, X., & Bronaugh, D. (2013). Climate extremes indices in the CMIP5 multimodel ensemble: Part 2. Future climate projections. *Journal of Geophysical Research: Atmospheres*, *118*(6), 2473–2493. https://doi.org/10.1002/jgrd.50188

Silva, A., Neves, R., & de Brito, J. (2014). Statistical modelling of carbonation in reinforced concrete. *Cement and Concrete Composites*, *50*, 73–81. https://doi.org/10.1016/j.cemconcomp.2013.12.001

Smoyer-Tomic, K. E., & Rainham, D. G. C. (2001). Beating the heat: development and evaluation of a Canadian hot weather health-response plan. (Articles). *Environmental Health*

Perspectives, *109*(12), 1241-. Retrieved from http://link.gale.com/apps/doc/A82551832/EAIM?u=usaskmain&sid=zotero&xid=959742ab

Stewart, M. G., Wang, X., & Nguyen, M. N. (2011). Climate change impact and risks of concrete infrastructure deterioration. *Engineering Structures*, *33*(4), 1326–1337. https://doi.org/10.1016/j.engstruct.2011.01.010

Tang, G., Clark, M. P., Newman, A. J., Wood, A. W., Papalexiou, S. M., Vionnet, V., & Whitfield, P. H. (2020). SCDNA: a serially complete precipitation and temperature dataset for North America from 1979 to 2018. *Earth System Science Data*, *12*(4), 2381–2409. https://doi.org/10.5194/essd-12-2381-2020

Tang, U. W., & Wang, Z. S. (2007). Influences of urban forms on traffic-induced noise and air pollution: Results from a modelling system. *Environmental Modelling & Software*, *22*(12), 1750–1764. https://doi.org/10.1016/j.envsoft.2007.02.003

Tebaldi, C., & Knutti, R. (2007). The use of the multi-model ensemble in probabilistic climate projections. *Philosophical Transactions of the Royal Society A: Mathematical, Physical and Engineering Sciences*, *365*(1857), 2053–2075. https://doi.org/10.1098/rsta.2007.2076

Terink, W., Hurkmans, R. T. W. L., Torfs, P. J. J. F., & Uijlenhoet, R. (2010). Evaluation of a bias correction method applied to downscaled precipitation and temperature reanalysis for the Rhine basin. *Hydrology and Earth System Sciences*, *14*(4), 687–703. https://doi.org/10.5194/hess-14-687-2010

Teutschbein, C., & Seibert, J. (2012). Bias correction of regional climate model simulations for hydrological climate-change impact studies: Review and evaluation of different methods.

Journal of Hydrology, *456–457*, 12–29. https://doi.org/10.1016/j.jhydrol.2012.05.052

Thrasher, B., Maurer, E. P., McKellar, C., & Duffy, P. B. (2012). Technical Note: Bias correcting climate model simulated daily temperature extremes with quantile mapping. *Hydrology and Earth System Sciences*, *16*(9), 3309. Retrieved from http://link.gale.com/apps/doc/A481466919/EAIM?u=usaskmain&sid=zotero&xid=93e37ec8

Urban, M. C., Bocedi, G., Hendry, A. P., Mihoub, J.-B., Pe'er, G., Singer, A., et al. (2016). Improving the forecast for biodiversity under climate change. *Science*, *353*(6304). https://doi.org/10.1126/science.aad8466

Wang, J., Zhan, Q., & Guo, H. (2016). The Morphology, Dynamics and Potential Hotspots of Land Surface Temperature at a Local Scale in Urban Areas. *Remote Sensing*, *8*(1), 18. https://doi.org/10.3390/rs8010018

Weaver, A. J. (2003). The Science of Climate Change. *Geoscience Canada*. Retrieved from https://journals.lib.unb.ca/index.php/GC/article/view/4147

Wicki, A., & Parlow, E. (2017). Multiple Regression Analysis for Unmixing of Surface Temperature Data in an Urban Environment. *Remote Sensing*, *9*(7), 684. https://doi.org/10.3390/rs9070684

Zhang, X., Alexander, L., Hegerl, G. C., Jones, P., Tank, A. K., Peterson, T. C., et al. (2011). Indices for monitoring changes in extremes based on daily temperature and precipitation data. *WIREs Climate Change*, *2*(6), 851–870. https://doi.org/10.1002/wcc.147

Zhou, X., Huang, G., Wang, X., Fan, Y., & Cheng, G. (2018). A coupled dynamical-copula downscaling approach for temperature projections over the Canadian Prairies. *Climate*

Dynamics, *51*(7), 2413–2431. https://doi.org/10.1007/s00382-017-4020-3

Chapter-3: Summary and Recommendation for future work

3.1 Summary and general discussion

Strategies for adaption to increased temperature projections rely on resilient urban-based projections, despite are uncertainties associated with atmospheric processes and climate models that generate futuristic temperature. Hence a combination of the use of four emission scenarios, that are all possible, and bias-correcting the future data gives the best opportunity to identify projected changes and makes the information more relevant to planners and decision-makers who are faced with adaptation at a local or regional scale, like large urban centers. The applications of reliable climate projections are multi-fold in Canadian cities; the extreme temperature will lead to higher extreme events such as heatwaves, storms and droughts, and all provincial governments in Canada have some form of climate contingency plans for the future as a result of the projections (Li et al., 2018).

Emission scenarios help understand climate projections better, and provide a comprehensive coverage and possibilities of understanding temperature projections. Amongst the emission scenarios the most optimistic scenario (SSP1-2.6), did exhibit a decreasing temperature and correspondingly decreasing absolute annual maximum and minimum temperatures, and even decreasing threshold and duration trends. The projections through various extreme temperature indices across other scenarios show a steady increase in yearly maximum and minimum (Absolute indices), translating to a steady increase both duration and frequency of warmer temperatures across all Canadian cities (Seneviratne et al., 2016) The findings of temperature indices align with the previous multi-decadal temperature based projections studies (Gaur et al., 2018; Power et al., 2017; Zhou et al., 2018). The combined effects of extreme temperature indices will contribute to a combined increase in extreme weather events, consequentially increasing the risks of urban heat-related mortality rates (Martin et al., 2012). The trends exhibited by the temperature indices, depict a faster rate of increase of TN projection over TX projections, leading to higher changes in Annual minimum (TNn). Annual maximum and minimum temperature projections (TXx and TNn), are

higher than mean temperature projections of 2 °C by 2050 and 6-7°C by 2100. The results of TXx and TNn across emission scenarios show that the increase at the end of 2100 is between much higher, between 10°C - 14°C across the emission scenarios.

The spatial patterns are represented by the mean of the trend of all the models for a particular emission scenario for all the indices. The trends of absolute indices (TXx and TNn) shed light on the higher predicted increasing TX trends in the cities in the Canadian prairies and the Great Lakes regions. The trends align with previous research on the projections in the cities in the Canadian prairies. The cities are expected to warm faster than the rest of the country, and almost three-times that of the world's average (Sauchyn & Davidson, 2020). The increasing trends in absolute indices, can contribute to an even higher increase in prolonged heatwaves, by the end of the century in these climate regions (Fortune et al., 2013; Smoyer-Tomic & Rainham, 2001). The trend of absolute indices, is not consistent, the rate of increase of both the absolute indices, is the highest for the 2070-2100 decades. The percentage and the duration indices' spatial patterns also point towards a warming trend with the higher forcing or emission scenario (SSP5-8.5), The trend will be only be accentuated in larger urban centers that have already been grappling with negative implications of rising temperatures. Maximum temperature indices like TX90p and WSDI have a high increasing trend in coastal cities of Vancouver, Victoria and Halifax, pointing towards an even warmer climate, over the hot season in these cities in the higher emission scenarios (SSP3-7.0 and SSP5-8.5). The threshold indices also an indicator of warming trends especially in the cities in the prairies and the Great Lakes climate regions over the higher emission scenarios. The effects of harsh winters will still be persistent especially in these cities, but warmer spring and autumn is predicted by the increasing Icing days (ID) index, and marginal increase in Frost days (FD) over both these climatic regions.

Overall, the extreme temperature indices, exhibit a qualitative consistency in their trends between projections under different emission scenarios, with the trends in TX and TN projections. The results, corroborate the historical trends of temperature increase over many major cities in Canada. The frequency and duration of extreme temperature events, is predicted to increase, but there is more scope for even more extensive research on the frequency of other extreme events like floods, droughts and blizzards as a result of higher predicted maximum and minimum temperature increase in Canadian cities.

3.2 Applications of research topic

3.2.1 Role in UHI and mortality rates research

Reliant and robust climate-based projections have played a crucial role in assisting with adaptation and climate contingency programs all over the world. Relatively larger-scale climate projections provide observational evidence and hence helps with extensive understanding of the SUHI phenomenon(Gaur et al., 2018). Hence, large scale temperature projections focused on larger urban centers, can not only provide a foundation for assessment and research of urban heat islands. Although it is imperative for researchers to understand urban-rural temperature difference to make meaningful temperature projections, bias-corrected or downscaled projections also provide credible information for long-term urban planning and mitigation programs, for local authorities and city governments (Rizwan et al., 2008).

Continued research in temperature-related mortality studies, also relies on scenario-based temperature projection, to better understand the human susceptibility to higher ambient temperatures. Research in various bio-medical fields point towards negative consequences of higher temperatures, which not only include hyper and hypothermia but also long-term physiological changes to the human respiratory rate and circulation rate, contributing to higher mortality rates (Keatinge & Donaldson, 2004; Kolb et al., 2007). Modelling a relationship between mortality trends and meteorological conditions is a complex process. Previous research suggests that there is evidence to show that this relationship could be uncertain (McMichael et al., 2006). However, further research (Martin et al., 2012) does show increased mortality in Canadian cities with increased temp in IPCC's A2 scenario which is an intermediate scenario like SSP2-4.5. The research also pointed out that predicting future mortality rates, will need to account for uncertainty in temperature increase, which can be provided by using more climate models, and also various other emission scenarios (Martin et al., 2012). Hence, bias-corrected temperature projections for various Canadian cities, using a multi-model ensemble for various scenarios presents an opportunity for advancing current research in projecting mortality rates due to extreme temperature events in Canadian cities.

3.2.2 Role in assessing concrete deterioration

Deterioration of concrete structures, is a consequence of increasing concentration of atmospheric

CO_2. With about 1.1 trillion dollars invested in concrete infrastructure in developed countries comparable to the size of Australia (Stewart et al., 2011), rehabilitation of concrete structures could prove to be very expensive. Most concrete deterioration occurs, through either Carbonation or chloride ingress, both of which are not only dependent on the concentration of atmospheric CO_2, but also on ambient atmospheric temperature (Bastidas-Arteaga et al., 2010; Belda Revert et al., 2018). It is also understood that urban environments tend to contain 10-15% more CO_2 due to the 'heat-island' effect, which in-turn contributes to higher local ambient atmospheric temperature (Silva et al., 2014). Future projections can provide critical information to calculate the extent of corrosion, and in-turn help manage concrete infrastructure better in large cities. Carbonation deterioration risk studied in the Sydney, a city that has similar arid climate in some cities in Canada, was found to have increased by 400% (Stewart et al., 2011). Use of bias-corrected CMIP6 projections will provide scope for concrete deterioration assessment in Canadian cities, and can help with appropriate and cost-effective adaptation measures.

3.3 Recommendation for future work

The applications of CMIP6 temperature models are multi-fold, and offer a could offer a wide range of opportunities for further analysis. However, a few uncertainties are persistent with most GCM models, along with some internal variability and CMIP models also could carry uncertainties. A few uncertainties, that exist are model uncertainty; where the model could have a misrepresentation of its inbuilt dynamic and physical processes, and also scenario uncertainty, where the modelled projections of a scenario are not always consistent with the socio-economic conditions that prevail in communities across the world (Barrow & Sauchyn, 2017)

- Although, the thesis uses multiple CMIP6 models, the model performances are not qualitatively analyzed. Various models can be assessed through model performance indicators and model variance indicators (LUO et al., 2020)
- Although the thesis is based on extreme temperature events in Canada, through assessing extreme temperature indices, the research can be extended to projecting heat-waves and frameworks for adaptation and mitigation strategies.
- The thesis not only offers scope for urban-heat island research but is also extremely helpful for research urban-planning and mitigation measures. Research on building

frameworks to tackle the SUHI effect, is a way forward for UHI research.

- The use of CMIP6 models to evaluate extreme temperature indices need not be restricted to use for Canadian cities, but for entire region of Canada. The use of other reliable gridded observation or reanalysis datasets can be used, for bias-correction or downscaling processes.
- Extreme events using TX or TN datasets cannot be simulated with high accuracy in a smaller spatial scale using downscaling processes. Hence statistical or dynamic downscaling processes can be applied on CMIP6 models across emission scenarios for varied perspective on projections across Canadian cities.

References

Alexander, L. V., Zhang, X., Peterson, T. C., Caesar, J., Gleason, B., Tank, A. M. G. K., et al. (2006). Global observed changes in daily climate extremes of temperature and precipitation. *Journal of Geophysical Research: Atmospheres*, *111*(D5). https://doi.org/10.1029/2005JD006290

Allen, S. M. J., Gough, W. A., & Mohsin, T. (2015). Changes in the frequency of extreme temperature records for Toronto, Ontario, Canada. *Theoretical and Applied Climatology*, *119*(3), 481–491. https://doi.org/10.1007/s00704-014-1131-1

Anandhi, A., Frei, A., Pierson, D. C., Schneiderman, E. M., Zion, M. S., Lounsbury, D., & Matonse, A. H. (2011). Examination of change factor methodologies for climate change impact assessment. *Water Resources Research*, *47*(3). https://doi.org/10.1029/2010WR009104

Ashour, S. K., & Abdel-hameed, M. A. (2010). Approximate skew normal distribution. *Journal of Advanced Research*, *1*(4), 341–350. https://doi.org/10.1016/j.jare.2010.06.004

Azzalini, A. (2011). Skew-Normal Distribution. In M. Lovric (Ed.), *International Encyclopedia of Statistical Science* (pp. 1342–1344). Berlin, Heidelberg: Springer. https://doi.org/10.1007/978-3-642-04898-2_523

Barrow, E. M., & Sauchyn, D. J. (2017). An analysis of the performance of RCMs in simulating current climate over western Canada. *International Journal of Climatology*, *37*(S1), 640–658. https://doi.org/10.1002/joc.5028

Bastidas-Arteaga, E., Chateauneuf, A., Sánchez-Silva, M., Bressolette, Ph., & Schoefs, F. (2010). Influence of weather and global warming in chloride ingress into concrete: A stochastic

approach. *Structural Safety*, *32*(4), 238–249. https://doi.org/10.1016/j.strusafe.2010.03.002

Belda Revert, A., De Weerdt, K., Hornbostel, K., & Geiker, M. R. (2018). Carbonation-induced corrosion: Investigation of the corrosion onset. *Construction and Building Materials*, *162*, 847–856. https://doi.org/10.1016/j.conbuildmat.2017.12.066

Bonsal, B. R., Zhang, X., Vincent, L. A., & Hogg, W. D. (2001). Characteristics of Daily and Extreme Temperatures over Canada. *Journal of Climate*, *14*(9), 1959–1976. https://doi.org/10.1175/1520-0442(2001)014<1959:CODAET>2.0.CO;2

Buishand, T. A., & Brandsma, T. (1999). Dependence of precipitation on temperature at Florence and Livorno (Italy). *Climate Research*, *12*(1), 53–63. Retrieved from http://www.jstor.org/stable/24865998

Bush,E & Flato,G. (2019). *Canada's Changing Climate Report*. Natural Resources Canada. Retrieved from https://www.nrcan.gc.ca/climate-change/impacts-adaptations/canadas-changing-climate-report/21177

Cannon, A. J., Sobie, S. R., & Murdock, T. Q. (2015). Bias Correction of GCM Precipitation by Quantile Mapping: How Well Do Methods Preserve Changes in Quantiles and Extremes? *Journal of Climate*, *28*(17), 6938–6959. https://doi.org/10.1175/JCLI-D-14-00754.1

Chen, J., Brissette, F. P., Chaumont, D., & Braun, M. (2013). Finding appropriate bias correction methods in downscaling precipitation for hydrologic impact studies over North America. *Water Resources Research*, *49*(7), 4187–4205. https://doi.org/10.1002/wrcr.20331

Choi, Y.-Y., Suh, M.-S., & Park, K.-H. (2014). Assessment of Surface Urban Heat Islands over Three Megacities in East Asia Using Land Surface Temperature Data Retrieved from

COMS. *Remote Sensing*, *6*(6), 5852–5867. https://doi.org/10.3390/rs6065852

Daniel, M., Lemonsu, A., Déqué, M., Somot, S., Alias, A., & Masson, V. (2019). Benefits of explicit urban parameterization in regional climate modeling to study climate and city interactions. *Climate Dynamics*, *52*(5), 2745–2764. https://doi.org/10.1007/s00382-018-4289-x

Dave Sauchyn & Debra Davidson. (2020). *Canada in a Changing Climate: Regional Perspectives Report* (p. 72).

Diffenbaugh, N. S., & Giorgi, F. (2012). Climate change hotspots in the CMIP5 global climate model ensemble. *Climatic Change*, *114*(3), 813–822. https://doi.org/10.1007/s10584-012-0570-x

Ehret, U., Zehe, E., Wulfmeyer, V., Warrach-Sagi, K., & Liebert, J. (2012). HESS Opinions "Should we apply bias correction to global and regional climate model data?" *Hydrology and Earth System Sciences*, *16*(9), 3391–3404. https://doi.org/10.5194/hess-16-3391-2012

Eyring, V., Bony, S., Meehl, G. A., Senior, C. A., Stevens, B., Stouffer, R. J., & Taylor, K. E. (2016). Overview of the Coupled Model Intercomparison Project Phase 6 (CMIP6) experimental design and organization. *Geoscientific Model Development*, *9*(5), 1937–1958. https://doi.org/10.5194/gmd-9-1937-2016

Fortune, M. K., Mustard, C. A., Etches, J. J. C., & Chambers, A. G. (2013). Work-attributed Illness Arising From Excess Heat Exposure in Ontario, 2004–2010. *Canadian Journal of Public Health*, *104*(5), e420–e426. https://doi.org/10.17269/cjph.104.3984

Gallo, K., & Xian, G. (2014). Application of spatially gridded temperature and land cover data sets for urban heat island analysis. *Urban Climate*, *8*, 1–10.

https://doi.org/10.1016/j.uclim.2014.04.005

Gaur, A., Eichenbaum, M. K., & Simonovic, S. P. (2018). Analysis and modelling of surface Urban Heat Island in 20 Canadian cities under climate and land-cover change. *Journal of Environmental Management*, *206*, 145–157. https://doi.org/10.1016/j.jenvman.2017.10.002

Gosling, S. N., Lowe, J. A., McGregor, G. R., Pelling, M., & Malamud, B. D. (2009). Associations between elevated atmospheric temperature and human mortality: a critical review of the literature. *Climatic Change*, *92*(3), 299–341. https://doi.org/10.1007/s10584-008-9441-x

Government of Canada, S. C. (2015, April 13). Canada goes urban. Retrieved April 13, 2020, from https://www150.statcan.gc.ca/n1/pub/11-630-x/11-630-x2015004-eng.htm

Graham, L. P., Andréasson, J., & Carlsson, B. (2007). Assessing climate change impacts on hydrology from an ensemble of regional climate models, model scales and linking methods – a case study on the Lule River basin. *Climatic Change*, *81*(1), 293–307. https://doi.org/10.1007/s10584-006-9215-2

Grillakis, M. G., Koutroulis, A. G., & Tsanis, I. K. (2011). Climate change impact on the hydrology of Spencer Creek watershed in Southern Ontario, Canada. *Journal of Hydrology*, *409*(1), 1–19. https://doi.org/10.1016/j.jhydrol.2011.06.018

Grillakis, M. G., Koutroulis, A. G., Daliakopoulos, I. N., Tsanis, I. K., & Tsanis, I. K. (2017). A method to preserve trends in quantile mapping bias correction of climate modeled temperature. *Earth System Dynamics*, *8*, 889–900. https://doi.org/10.5194/esd-8-889-2017

Guo, L.-Y., Gao, Q., Jiang, Z.-H., & Li, L. (2018). Bias correction and projection of surface air temperature in LMDZ multiple simulation over central and eastern China. *Advances in*

Climate Change Research, *9*(1), 81–92. https://doi.org/10.1016/j.accre.2018.02.003

Haerter, J. O., Hagemann, S., Moseley, C., & Piani, C. (2011). Climate model bias correction and the role of timescales. *Hydrology and Earth System Sciences*, *15*(3), 1065–1079. https://doi.org/10.5194/hess-15-1065-2011

Ines, A. V. M., & Hansen, J. W. (2006). Bias correction of daily GCM rainfall for crop simulation studies. *Agricultural and Forest Meteorology*, *138*(1), 44–53. https://doi.org/10.1016/j.agrformet.2006.03.009

Jury, M. W., Prein, A. F., Truhetz, H., & Gobiet, A. (2015). Evaluation of CMIP5 Models in the Context of Dynamical Downscaling over Europe. *Journal of Climate*, *28*(14), 5575–5582. https://doi.org/10.1175/JCLI-D-14-00430.1

Katz, R. W., & Brown, B. G. (1992). Extreme events in a changing climate: Variability is more important than averages. *Climatic Change*, *21*(3), 289–302. https://doi.org/10.1007/BF00139728

Keatinge, W. R., & Donaldson, G. C. (2004, November). The impact of global warming on health and mortality. *Southern Medical Journal*, *97*(11), 1093+. Retrieved from http://link.gale.com/apps/doc/A126076453/EAIM?sid=bookmark-EAIM&xid=2396cc48

Knutti, R., & Sedláček, J. (2013). Robustness and uncertainties in the new CMIP5 climate model projections. *Nature Climate Change*, *3*(4), 369–373. https://doi.org/10.1038/nclimate1716

Kolb, S., Radon, K., Valois, M.-F., Héguy, L., & Goldberg, M. S. (2007). The Short-Term Influence of Weather on Daily Mortality in Congestive Heart Failure. *Archives of Environmental & Occupational Health*, *62*(4), 169–176. https://doi.org/10.3200/AEOH.62.4.169-176

Lauwaet, D., Hooyberghs, H., Maiheu, B., Lefebvre, W., Driesen, G., Looy, S. V., & Ridder, K. D. (2015). Detailed Urban Heat Island Projections for Cities Worldwide: Dynamical Downscaling CMIP5 Global Climate Models. *Climate*, *3*(2), 391–415. https://doi.org/10.3390/cli3020391

Li, H., Sheffield, J., & Wood, E. F. (2010). Bias correction of monthly precipitation and temperature fields from Intergovernmental Panel on Climate Change AR4 models using equidistant quantile matching. *Journal of Geophysical Research: Atmospheres*, *115*(D10). https://doi.org/10.1029/2009JD012882

Li, Z., Huang, G., Huang, W., Lin, Q., Liao, R., & Fan, Y. (2018). Future changes of temperature and heat waves in Ontario, Canada. *Theoretical and Applied Climatology*, *132*(3), 1029–1038. https://doi.org/10.1007/s00704-017-2123-8

LUO, N., GUO, Y., GAO, Z., CHEN, K., & CHOU, J. (2020). Assessment of CMIP6 and CMIP5 model performance for extreme temperature in China. *Atmospheric and Oceanic Science Letters*, *13*(6), 589–597. https://doi.org/10.1080/16742834.2020.1808430

Martin, S. L., Cakmak, S., Hebbern, C. A., Avramescu, M.-L., & Tremblay, N. (2012). Climate change and future temperature-related mortality in 15 Canadian cities. *International Journal of Biometeorology*, *56*(4), 605–619. https://doi.org/10.1007/s00484-011-0449-y

Maurer, E. P., Brekke, L., Pruitt, T., & Duffy, P. B. (2007). Fine-resolution climate projections enhance regional climate change impact studies. *Eos, Transactions American Geophysical Union*, *88*(47), 504–504. https://doi.org/10.1029/2007EO470006

McMichael, A. J., Woodruff, R. E., & Hales, S. (2006). Climate change and human health: present and future risks. *The Lancet*, *367*(9513), 859–869. https://doi.org/10.1016/S0140-

6736(06)68079-3

Meehl, G. A., & Tebaldi, C. (2004). More Intense, More Frequent, and Longer Lasting Heat Waves in the 21st Century. *Science*, *305*(5686), 994–997. Retrieved from https://www.jstor.org/stable/3837565

Murray, V., & Ebi, K. L. (2012). IPCC Special Report on Managing the Risks of Extreme Events and Disasters to Advance Climate Change Adaptation (SREX). *Journal of Epidemiology and Community Health (1979-)*, *66*(9), 759–760. Retrieved from http://www.jstor.org/stable/23269103

Notaro, M., Bennington, V., & Lofgren, B. (2015). Dynamical Downscaling-Based Projections of Great Lakes Water Levels*+. *Journal of Climate*, *28*(24), 9721–9745. https://doi.org/10.1175/JCLI-D-14-00847.1

Papalexiou, S. M., AghaKouchak, A., Trenberth, K. E., & Foufoula-Georgiou, E. (2018). Global, Regional, and Megacity Trends in the Highest Temperature of the Year: Diagnostics and Evidence for Accelerating Trends. *Earth's Future*, *6*(1), 71–79. https://doi.org/10.1002/2017EF000709

Peacock, S. (2012). Projected Twenty-First-Century Changes in Temperature, Precipitation, and Snow Cover over North America in CCSM4. *Journal of Climate*, *25*(13), 4405–4429. https://doi.org/10.1175/JCLI-D-11-00214.1

Pengelly, L. D., Campbell, M. E., Cheng, C. S., Fu, C., Gingrich, S. E., & Macfarlane, R. (2007). Anatomy of Heat Waves and Mortality in Toronto. *Canadian Journal of Public Health*, *98*(5), 364–368. https://doi.org/10.1007/BF03405420

Perkins, S. E., & Alexander, L. V. (2013). On the Measurement of Heat Waves. *Journal of Climate*,

26(13), 4500–4517. https://doi.org/10.1175/JCLI-D-12-00383.1

Piani, C., Weedon, G. P., Best, M., Gomes, S. M., Viterbo, P., Hagemann, S., & Haerter, J. O. (2010). Statistical bias correction of global simulated daily precipitation and temperature for the application of hydrological models. *Journal of Hydrology*, *395*(3), 199–215. https://doi.org/10.1016/j.jhydrol.2010.10.024

Piao, S., Ciais, P., Huang, Y., Shen, Z., Peng, S., Li, J., et al. (2010). The impacts of climate change on water resources and agriculture in China. *Nature*, *467*(7311), 43–51. https://doi.org/10.1038/nature09364

Plummer, D. A., Caya, D., Frigon, A., Côté, H., Giguère, M., Paquin, D., et al. (2006). Climate and Climate Change over North America as Simulated by the Canadian RCM. *Journal of Climate*, *19*(13), 3112–3132. https://doi.org/10.1175/JCLI3769.1

Power, S., Delage, F., Wang, G., Smith, I., & Kociuba, G. (2017). Apparent limitations in the ability of CMIP5 climate models to simulate recent multi-decadal change in surface temperature: implications for global temperature projections. *Climate Dynamics*, *49*(1), 53–69. https://doi.org/10.1007/s00382-016-3326-x

Reichstein, M., Bahn, M., Ciais, P., Frank, D., Mahecha, M. D., Seneviratne, S. I., et al. (2013). Climate extremes and the carbon cycle. *Nature*, *500*(7462), 287–295. https://doi.org/10.1038/nature12350

Rizwan, A. M., Dennis, L. Y. C., & Liu, C. (2008). A review on the generation, determination and mitigation of Urban Heat Island. *Journal of Environmental Sciences*, *20*(1), 120–128. https://doi.org/10.1016/S1001-0742(08)60019-4

Rummukainen, M. (2010). State-of-the-art with regional climate models. *WIREs Climate Change*,

1(1), 82–96. https://doi.org/10.1002/wcc.8

Schar, C., Vidale, P. L., Luthi, D., Frei, C., Haberli, C., Liniger, M. A., & Appenzeller, C. (2004). The role of increasing temperature variability in European summer heatwaves. *Nature*, *427*(6972), 332-. Retrieved from http://link.gale.com/apps/doc/A186371710/EAIM?u=usaskmain&sid=zotero&xid=e5e58c2c

Seneviratne, S. I., Donat, M. G., Pitman, A. J., Knutti, R., & Wilby, R. L. (2016). Allowable CO 2 emissions based on regional and impact-related climate targets. *Nature*, *529*(7587), 477–483. https://doi.org/10.1038/nature16542

Sillmann, J., Kharin, V. V., Zhang, X., Zwiers, F. W., & Bronaugh, D. (2013). Climate extremes indices in the CMIP5 multimodel ensemble: Part 1. Model evaluation in the present climate. *Journal of Geophysical Research: Atmospheres*, *118*(4), 1716–1733. https://doi.org/10.1002/jgrd.50203

Sillmann, J., Kharin, V. V., Zwiers, F. W., Zhang, X., & Bronaugh, D. (2013). Climate extremes indices in the CMIP5 multimodel ensemble: Part 2. Future climate projections. *Journal of Geophysical Research: Atmospheres*, *118*(6), 2473–2493. https://doi.org/10.1002/jgrd.50188

Silva, A., Neves, R., & de Brito, J. (2014). Statistical modelling of carbonation in reinforced concrete. *Cement and Concrete Composites*, *50*, 73–81. https://doi.org/10.1016/j.cemconcomp.2013.12.001

Smoyer-Tomic, K. E., & Rainham, D. G. C. (2001). Beating the heat: development and evaluation of a Canadian hot weather health-response plan. (Articles). *Environmental Health*

Perspectives, *109*(12), 1241-. Retrieved from http://link.gale.com/apps/doc/A82551832/EAIM?u=usaskmain&sid=zotero&xid=959742ab

Stewart, M. G., Wang, X., & Nguyen, M. N. (2011). Climate change impact and risks of concrete infrastructure deterioration. *Engineering Structures*, *33*(4), 1326–1337. https://doi.org/10.1016/j.engstruct.2011.01.010

Tang, G., Clark, M. P., Newman, A. J., Wood, A. W., Papalexiou, S. M., Vionnet, V., & Whitfield, P. H. (2020). SCDNA: a serially complete precipitation and temperature dataset for North America from 1979 to 2018. *Earth System Science Data*, *12*(4), 2381–2409. https://doi.org/10.5194/essd-12-2381-2020

Tang, U. W., & Wang, Z. S. (2007). Influences of urban forms on traffic-induced noise and air pollution: Results from a modelling system. *Environmental Modelling & Software*, *22*(12), 1750–1764. https://doi.org/10.1016/j.envsoft.2007.02.003

Tebaldi, C., & Knutti, R. (2007). The use of the multi-model ensemble in probabilistic climate projections. *Philosophical Transactions of the Royal Society A: Mathematical, Physical and Engineering Sciences*, *365*(1857), 2053–2075. https://doi.org/10.1098/rsta.2007.2076

Terink, W., Hurkmans, R. T. W. L., Torfs, P. J. J. F., & Uijlenhoet, R. (2010). Evaluation of a bias correction method applied to downscaled precipitation and temperature reanalysis for the Rhine basin. *Hydrology and Earth System Sciences*, *14*(4), 687–703. https://doi.org/10.5194/hess-14-687-2010

Teutschbein, C., & Seibert, J. (2012). Bias correction of regional climate model simulations for hydrological climate-change impact studies: Review and evaluation of different methods.

Journal of Hydrology, *456–457*, 12–29. https://doi.org/10.1016/j.jhydrol.2012.05.052

Thrasher, B., Maurer, E. P., McKellar, C., & Duffy, P. B. (2012). Technical Note: Bias correcting climate model simulated daily temperature extremes with quantile mapping. *Hydrology and Earth System Sciences*, *16*(9), 3309. Retrieved from http://link.gale.com/apps/doc/A481466919/EAIM?u=usaskmain&sid=zotero&xid=93e37ec8

Urban, M. C., Bocedi, G., Hendry, A. P., Mihoub, J.-B., Pe'er, G., Singer, A., et al. (2016). Improving the forecast for biodiversity under climate change. *Science*, *353*(6304). https://doi.org/10.1126/science.aad8466

Wang, J., Zhan, Q., & Guo, H. (2016). The Morphology, Dynamics and Potential Hotspots of Land Surface Temperature at a Local Scale in Urban Areas. *Remote Sensing*, *8*(1), 18. https://doi.org/10.3390/rs8010018

Weaver, A. J. (2003). The Science of Climate Change. *Geoscience Canada*. Retrieved from https://journals.lib.unb.ca/index.php/GC/article/view/4147

Wicki, A., & Parlow, E. (2017). Multiple Regression Analysis for Unmixing of Surface Temperature Data in an Urban Environment. *Remote Sensing*, *9*(7), 684. https://doi.org/10.3390/rs9070684

Zhang, X., Alexander, L., Hegerl, G. C., Jones, P., Tank, A. K., Peterson, T. C., et al. (2011). Indices for monitoring changes in extremes based on daily temperature and precipitation data. *WIREs Climate Change*, *2*(6), 851–870. https://doi.org/10.1002/wcc.147

Zhou, X., Huang, G., Wang, X., Fan, Y., & Cheng, G. (2018). A coupled dynamical-copula downscaling approach for temperature projections over the Canadian Prairies.

Appendix: Chapter 1 Supplementary Information

Table A.1: Future Model Scenarios used for CMIP6

Tier 1 Scenarios	Forcing Category	2100 Forcing W m-2	# of SSP
SSP5-8.5	High	8.5	5
SSP3-7.0	High	7	3
SSP2-4.5	Medium	4.5	2
SSP1-2.6	Low	2.6	1

Table A.2: List of cities with historical trend.

City Name	Population Growth (1980-2020)	Area(km²)	Elevation(m)	Slope of SCDNA (°C/year)
Toronto	3247000	7124	85	0.0548
Montreal	1423000	4258	40	0.0692
Vancouver	1359000	2700	31	-0.0035
Calgary	1013000	825	1050	0.0085
Edmonton	985227	684	645	0.0093
Ottawa-Gatineau	679000	2790	70	0.1919
Winnipeg	244000	464	239	0.0218
Quebec City	264000	484	98	0.0376
Hamilton	227000	1138	324	0.0308
Kitchener	286000	136.9	301	0.0402
London	228000	1572	251	0.0370
Victoria	159000	19.47	23	0.0146

Halifax	137000	234.72	102	0.0407
Oshawa	256000	145.7	106	0.0440
Windsor	89000	146.3	190	0.0317
Saskatoon	181000	228.1	482	0.0086
St Catharines-Niagara Falls	113000	302.81	98	0.0359
Regina	101184	180	577	-0.0132

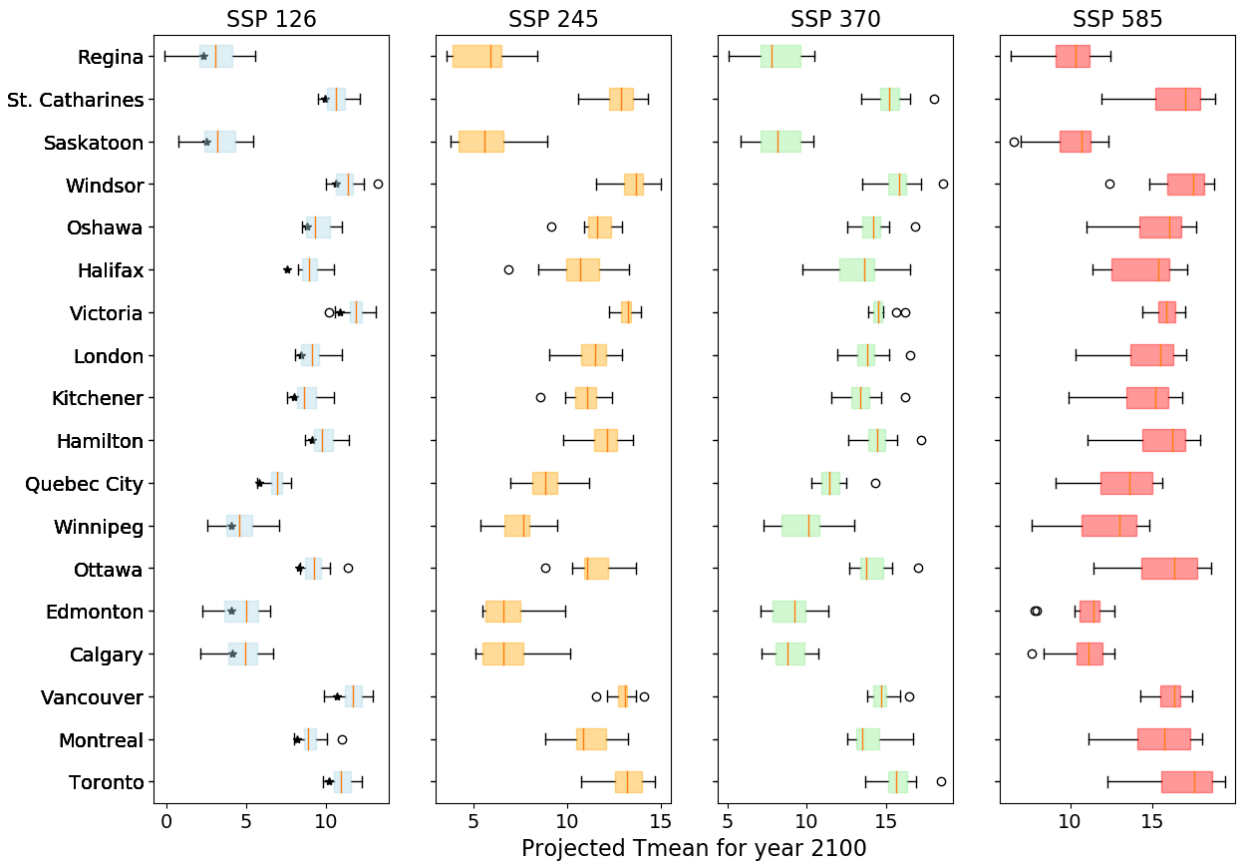

Figure A.1: Annual mean for all the CMIP6 models for the year 2100. The black star in the SSP1-2.6 boxplots, represents the annual historical mean (1979-2014) for all the cities.

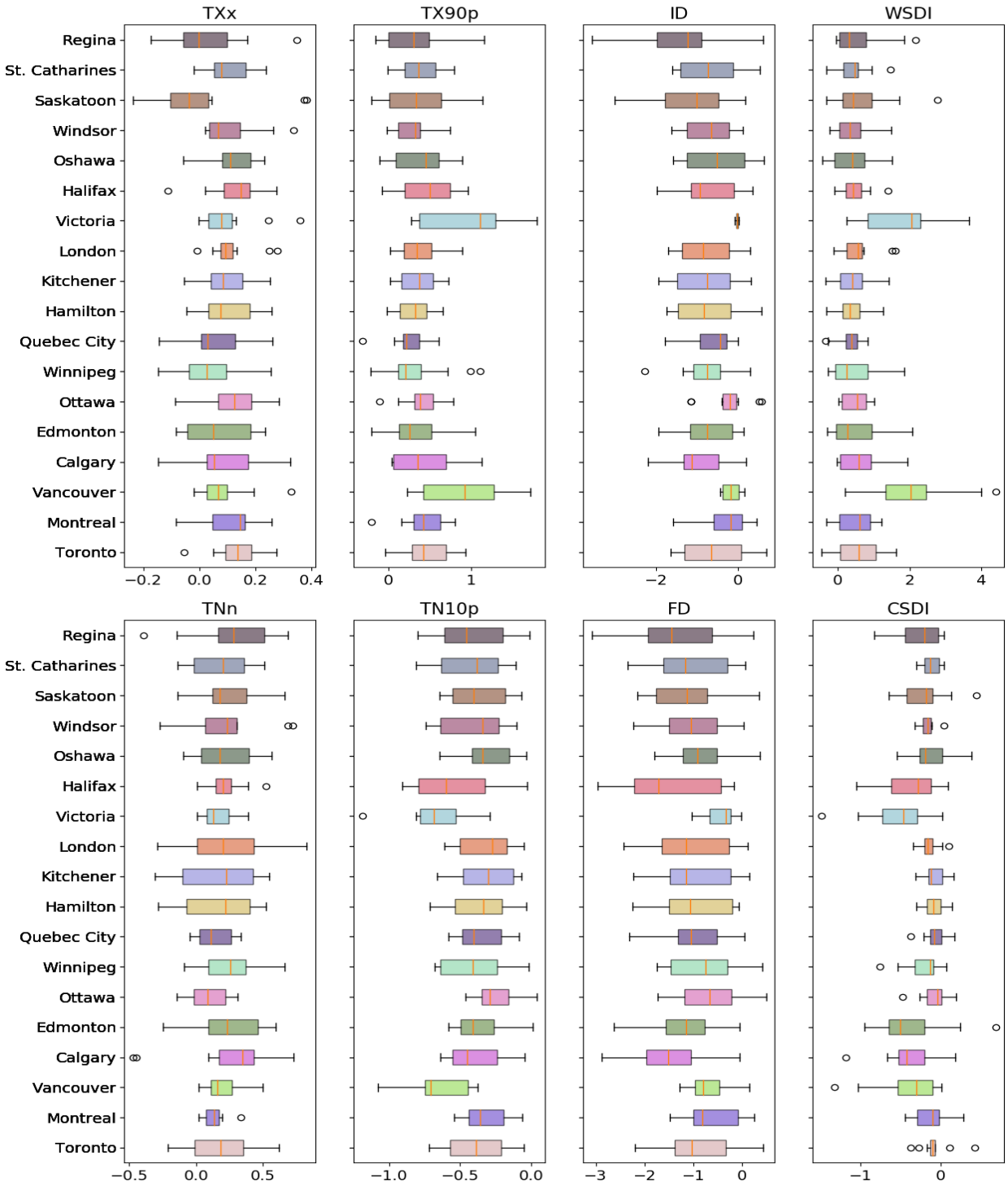

Figure A.2: Indices Slopes for CMIP6 models as shown for the emission scenario SSP1-2.6. The units of the indices are °C/decade for TXx and TNn, days/decade for WSDI, CSDI, ID and FD and %/decade for TX90p and TN10p.

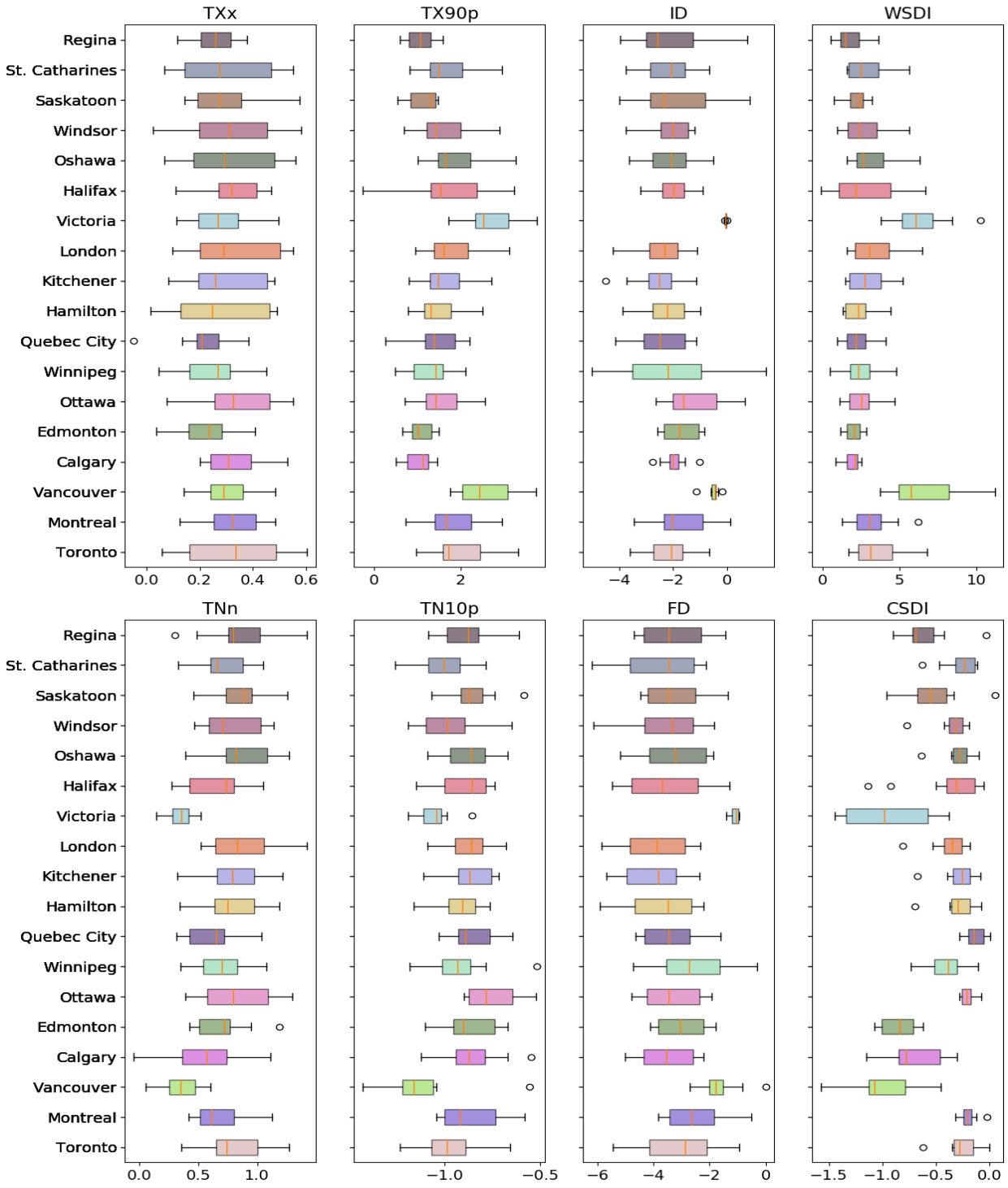

Figure A.3: Indices Slopes for CMIP6 models as shown for the emission scenario SSP2-4.5. The units of the indices are °C/decade for TXx and TNn, days/decade for WSDI, CSDI, ID and FD and %/decade for TX90p and TN10p.

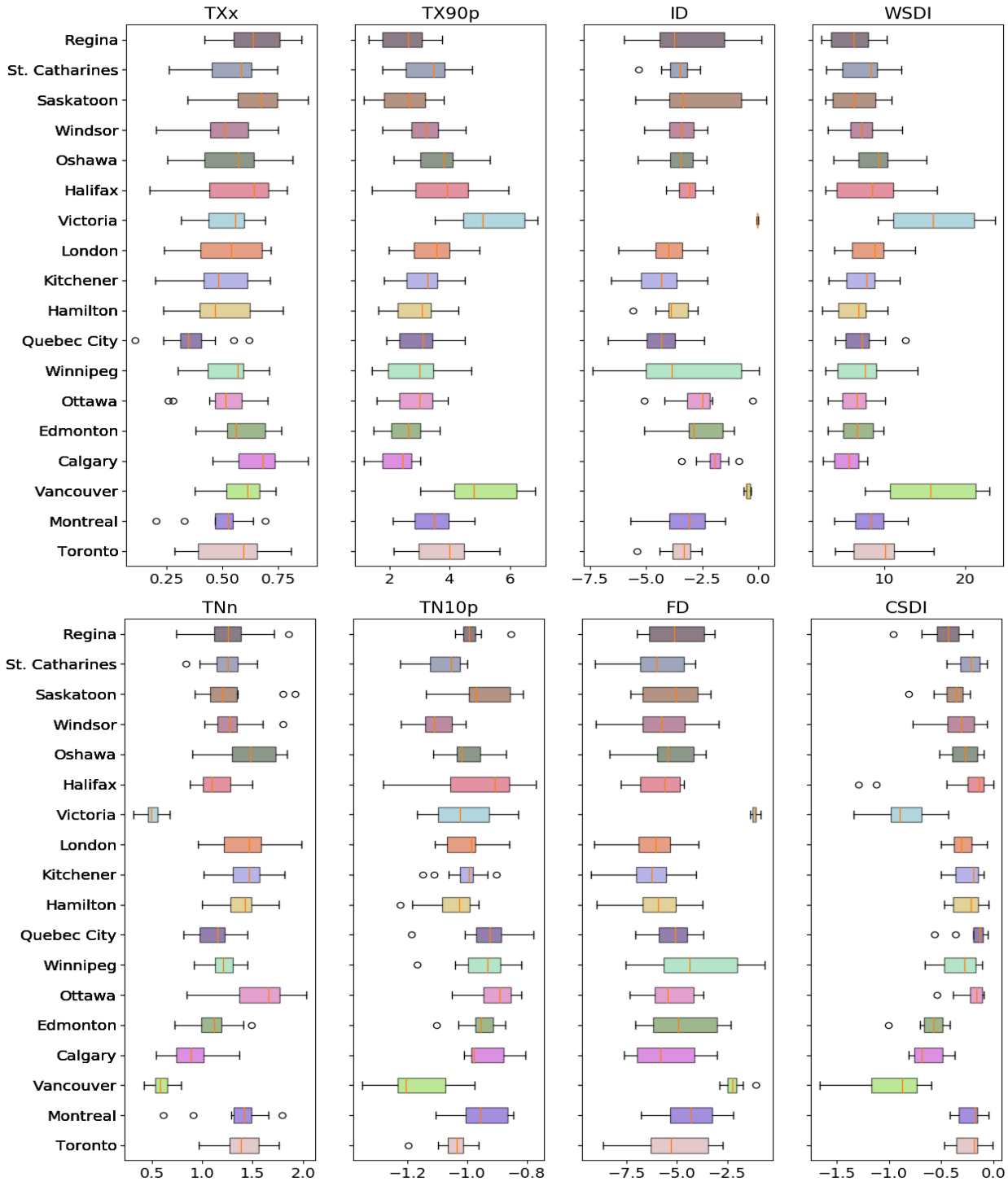

Figure A. 4: Indices Slopes for CMIP6 models as shown for the emission scenario SSP3-7.0. The units of the indices are °C/decade for TXx and TNn, days/decade for WSDI, CSDI, ID and FD and %/decade for TX90p and TN10p.

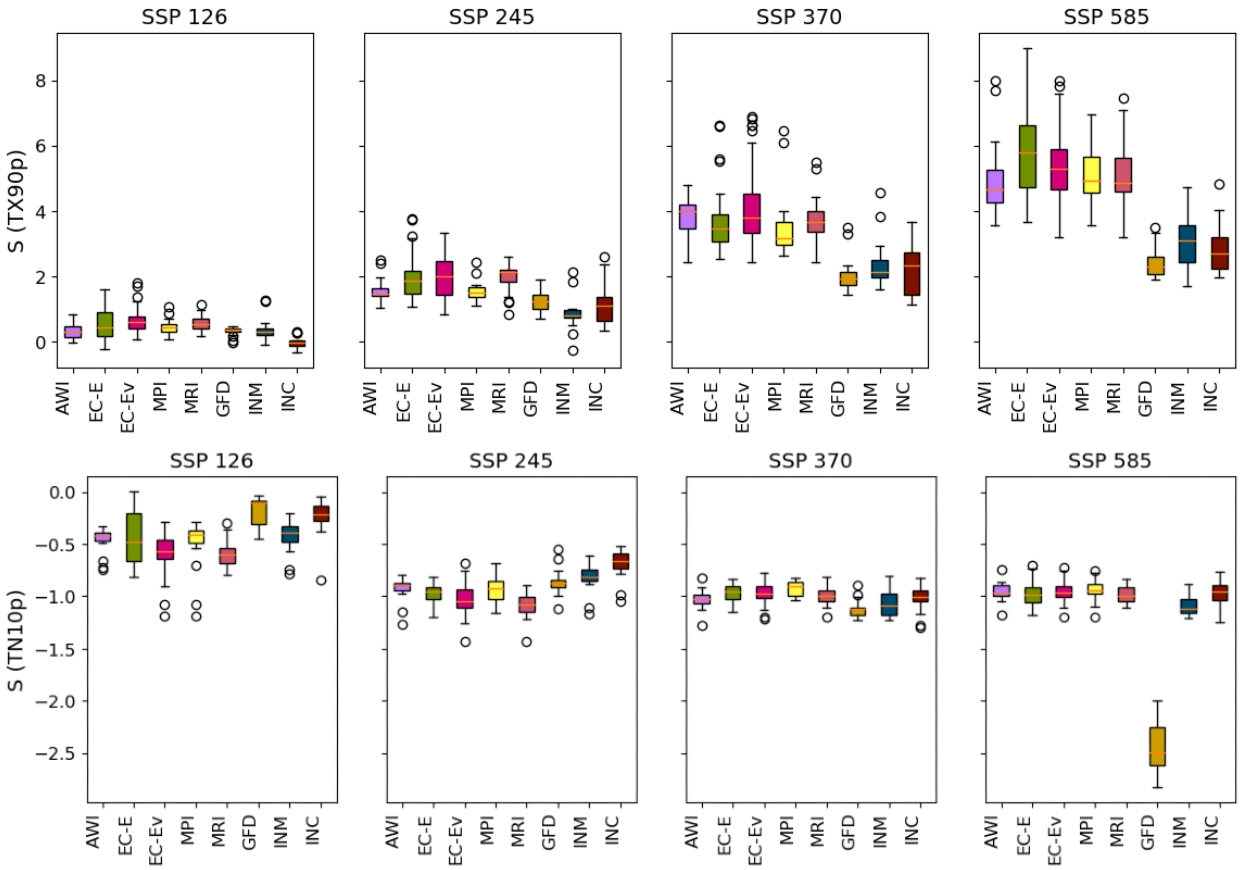

Figure A.5: Slopes of TX90p and TN10p indices for individual models (°C per year) for all emission scenarios. The units of the rate of change are °C/decade.

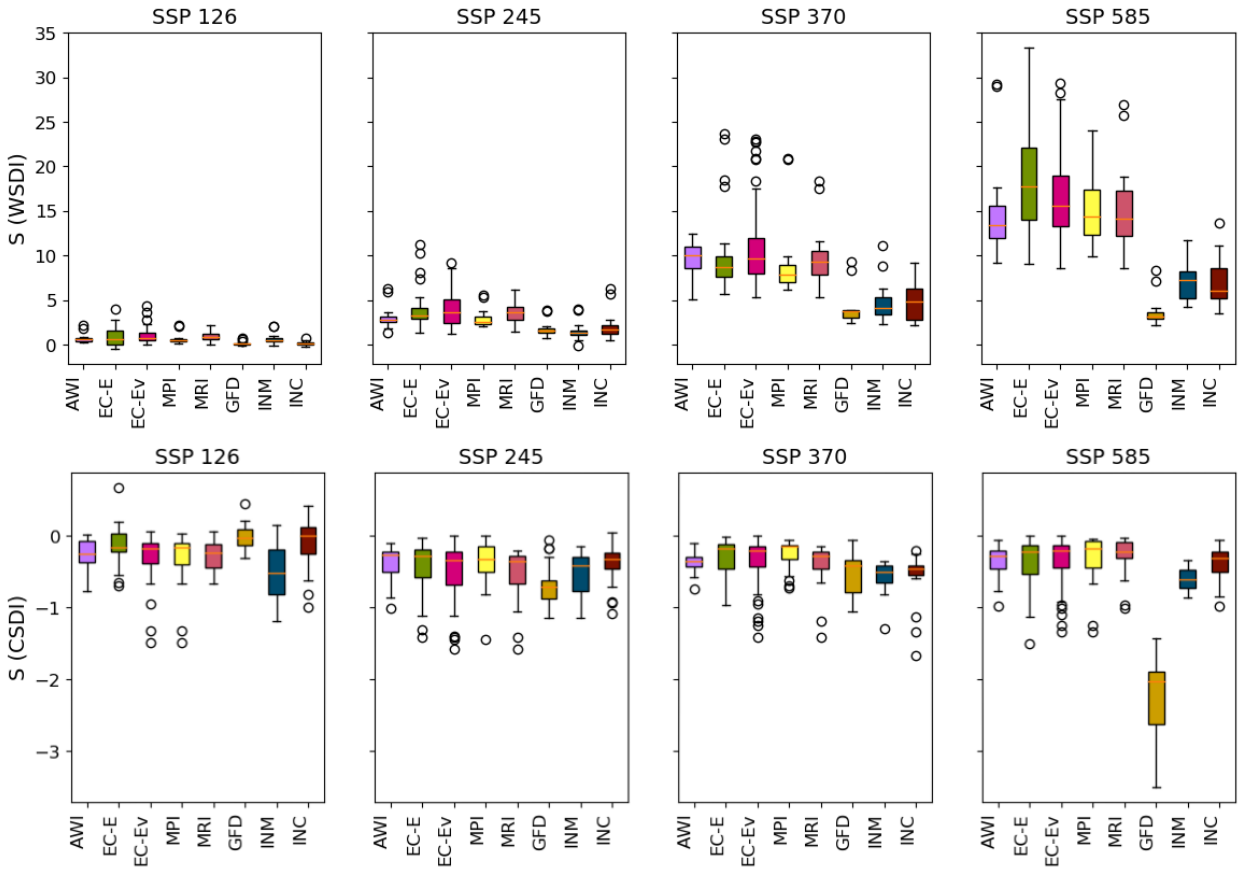

Figure A.6: Slopes of WSDI and CSDI indices for individual models for all emission scenarios. The units of the rate of change are days/decade.

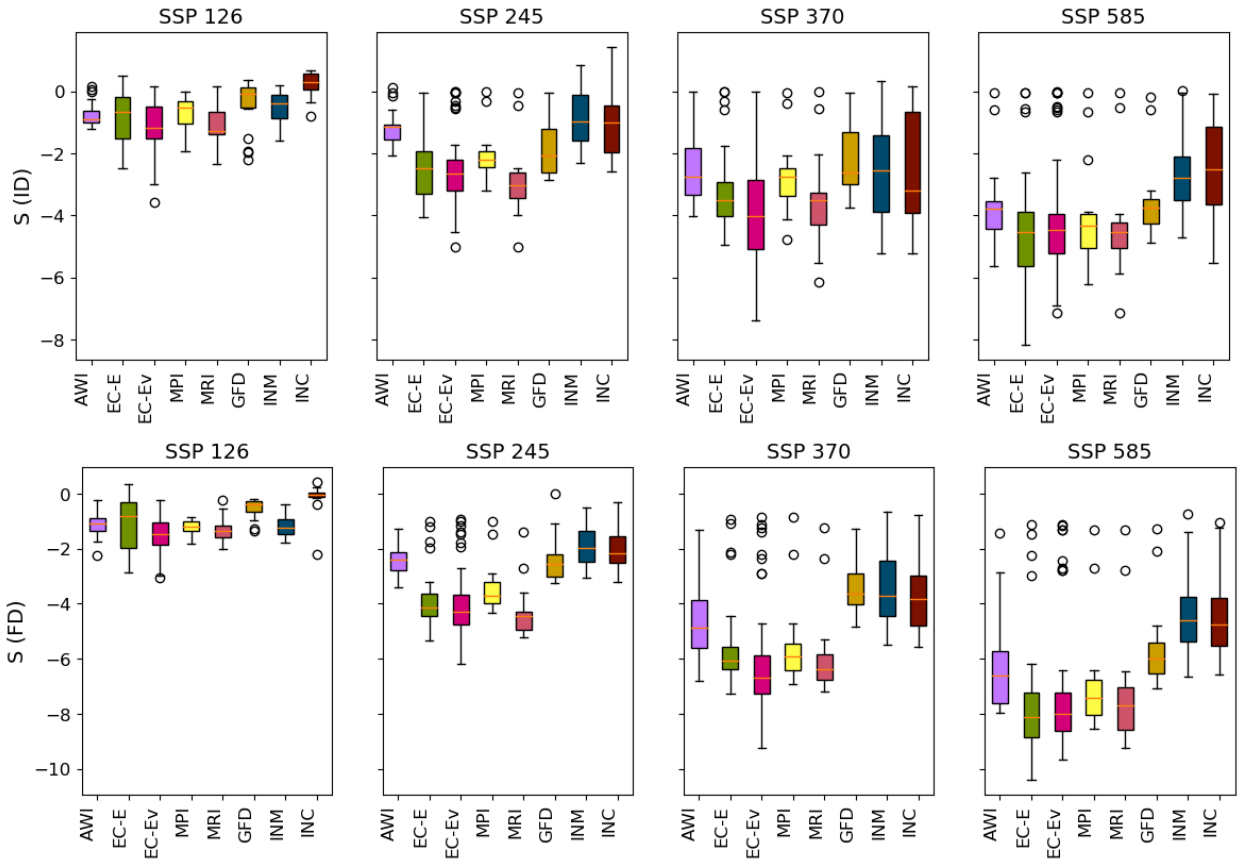

Figure A.7: Slopes of ID and FD indices for individual models for all emission scenarios. The units of the rate of change are days/decade.

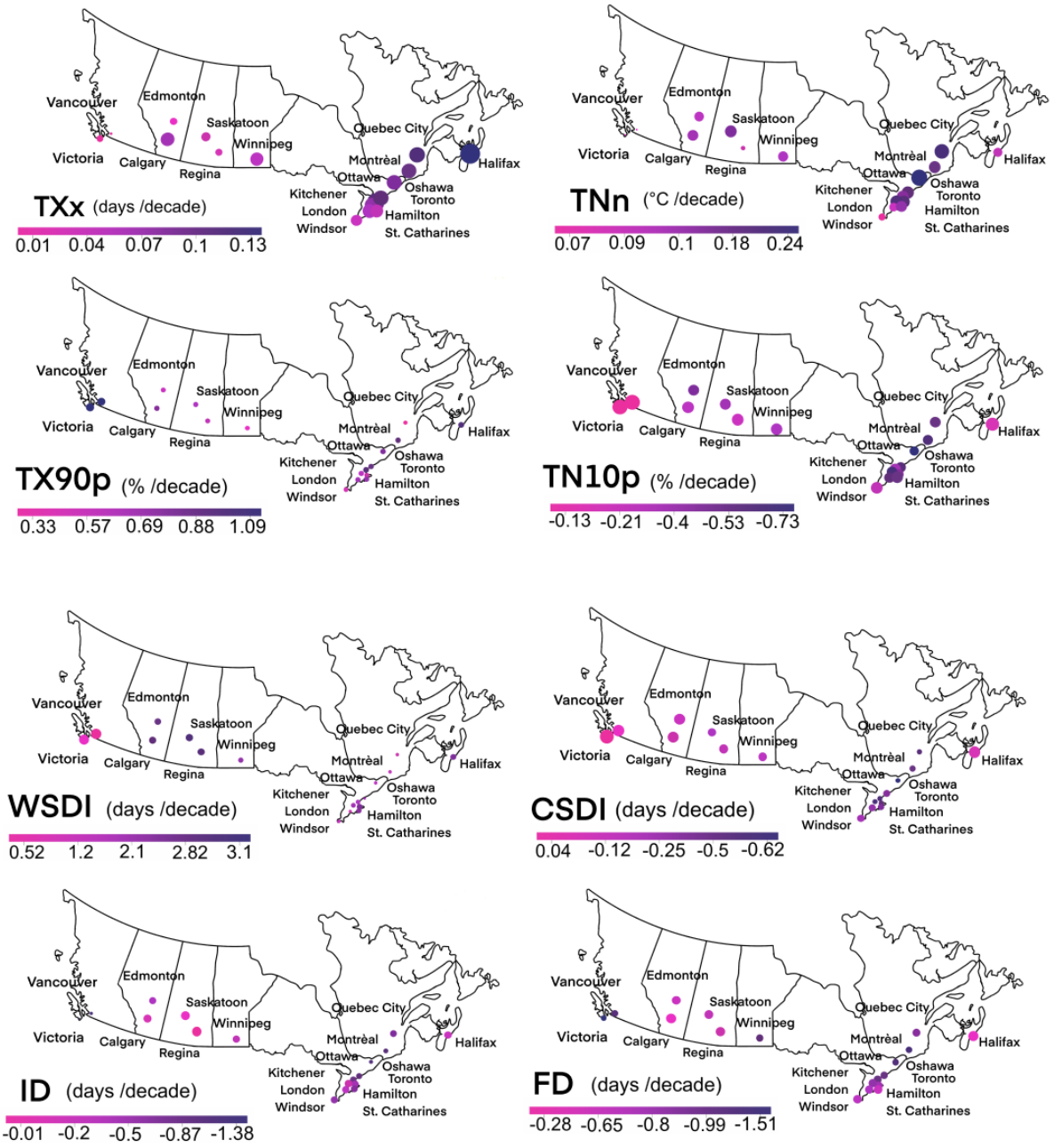

Figure A.8: Spatial trends variation of all 8 indices for the emission scenario SSP1-2.6. The size of the dots is proportional to the magnitude of the trend.

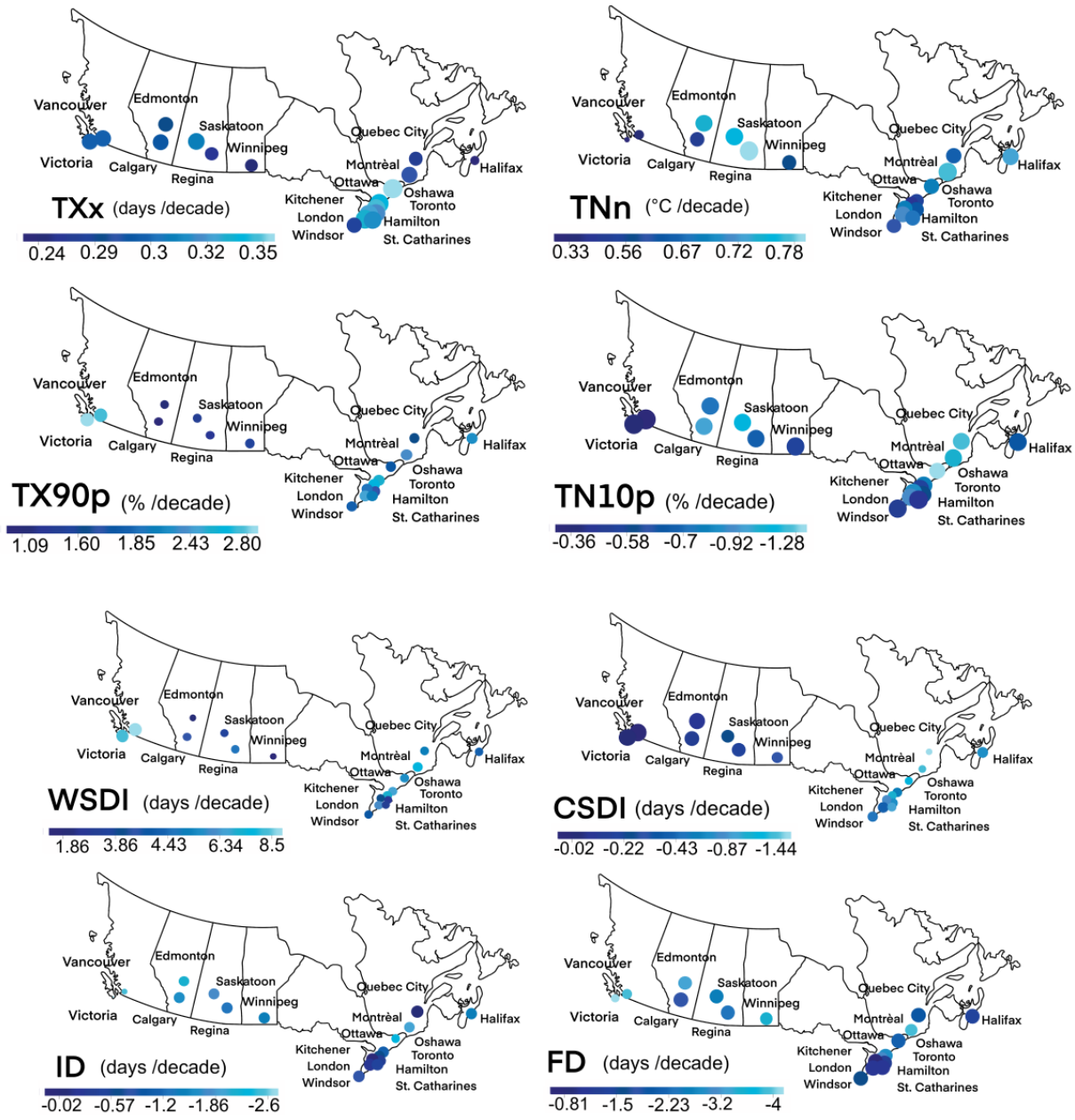

Figure A.9: Spatial trends variation of all 8 indices for the emission scenario SSP2-4.5. The size of the dots is proportional to the magnitude of the trend.

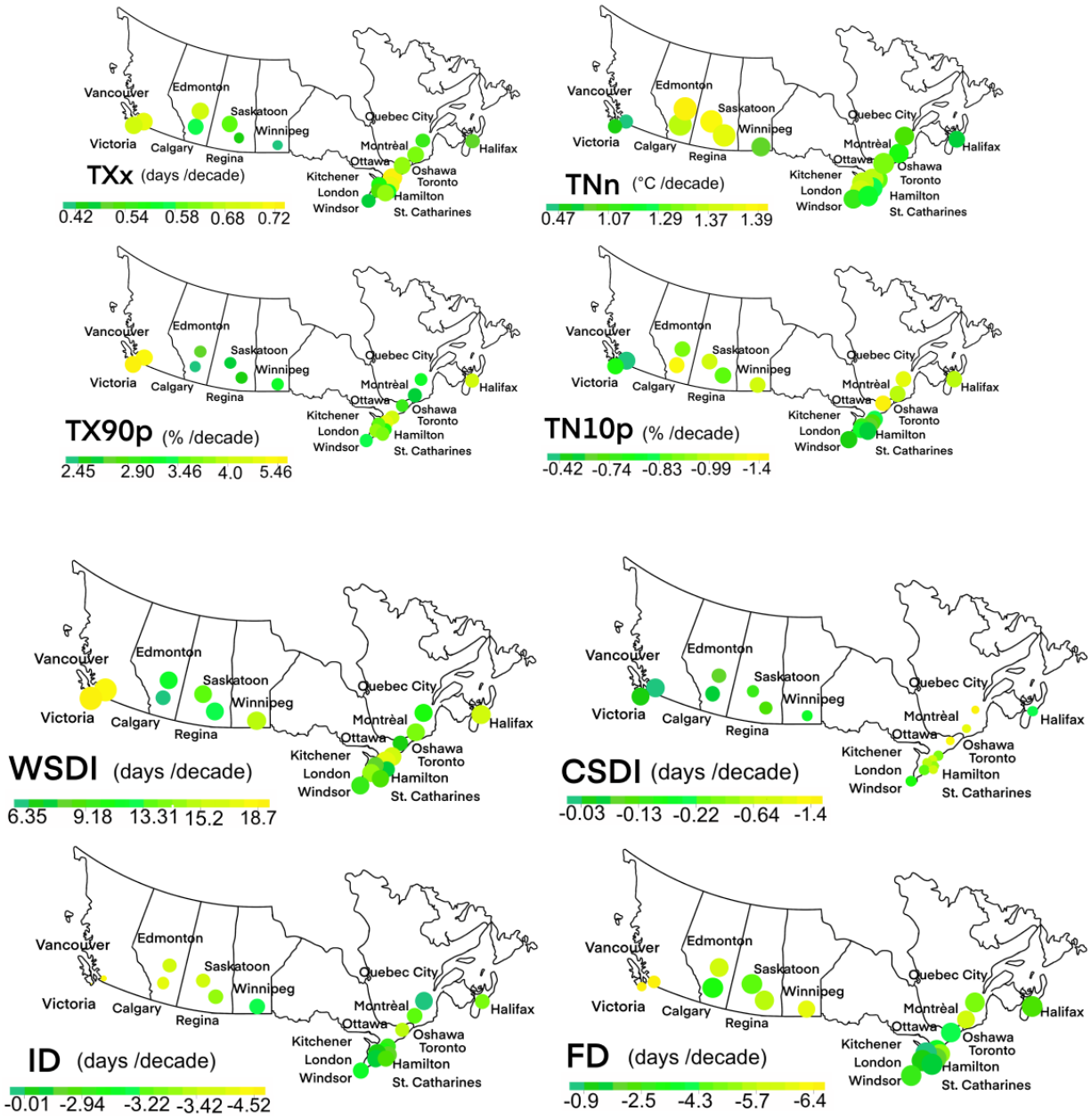

Figure A.10: Spatial trends variation of all 8 indices for the emission scenario SSP3-7.0. The size of the dots is proportional to the magnitude of the trend.